On the evaluation of decay curves to determine structural reverberation times for building elements

C. Hopkins and M. Robinson

Acoustics Research Unit, School of Architecture, University of Liverpool, Liverpool L69 7ZN, United Kingdom

E-mail for corresponding author: carl.hopkins@liv.ac.uk

Keywords: structural reverberation times, decay curve, sound transmission, transient statistical energy analysis, transmission suite, flanking laboratory

Abstract

Measurement of structural reverberation times on heavyweight walls and floors is often essential to accompany laboratory measurements of airborne or impact sound insulation, or to quantify vibration transmission on junctions of walls and floors. This paper uses Transient Statistical Energy Analysis (TSEA) to predict structural decay curves that can be evaluated to determine the structural reverberation time. Good agreement is shown between decay curves measured on concrete/masonry walls and floors in a large building and those predicted using TSEA. A series of numerical experiments are then performed with TSEA to quantify the error in the estimate of the total loss factor when using different evaluation ranges to calculate the structural reverberation time. The intention is to reconcile the three main issues that have historically caused problems when measuring structural reverberation times on heavyweight walls and floors. These issues are: (1) the evaluation range that is needed to ensure that the total loss factor calculated from the decay curve is representative of the true total loss factor, (2) the errors in the total loss factor when placed in the context of the other errors that occur due to energy flow between the test element and the connected structure, and (3) the signal processing that is necessary to measure and evaluate short decays. The outcome is a proposal for an evaluation procedure to determine structural reverberation times that maximises the part of the early decay which can be used in the evaluation range and identifies when a structural decay curve is and is not significantly affected by energy returning from the rest of the structure.

1. Introduction

In building acoustics, the measurement of structural reverberation times on walls and floors is often essential for both laboratory and field measurements. For transmission suite measurements the structural reverberation time is needed to compare the airborne or impact sound insulation of heavyweight walls and floors that have been measured in different laboratories where the boundary conditions differ, or to estimate the *in situ* performance of a wall or floor [1,2,3]. Structural reverberation times are also needed to calculate structural coupling parameters such as the vibration reduction index [4] or the coupling loss factor [3] from measurements on junctions of walls/floors in flanking laboratories or *in situ*.

The measured structural reverberation time is only useful if it provides an estimate of the total loss factor for the test element. Hence this element must be relatively homogeneous and support a reverberant bending wave field with no significant decrease in vibration level over the surface. Ideally, test elements would always be installed in a laboratory in such a way that the mean–square velocity of the excited element is inversely proportional to its total loss factor. However, this will not occur for many masonry/concrete walls and floors because the assumption that the bending wave energy associated with the test element remains only in the element, or only flows outwards into the connected structure, never to return, is not always valid. When the energy in the connected structure returns to the excited test element, the structural decay curve for the vibration level is not described by a straight line. To ensure that total loss factors calculated from structural reverberation times are appropriate for the uses described above, it is often considered appropriate to use 'short' evaluation ranges for the reverberation time so that the effect of energy returning to the test element from other parts of the connected structure is negligible [3,4].

Indications that the structure of a transmission suite can affect the structural reverberation time of the installed test element are found in Kling and Scholl [5] who used Transient Statistical Energy Analysis (TSEA) to model a Perspex scale model of a horizontal transmission suite. However the applicability of the findings to actual transmission suites is limited because the work omitted the

following aspects. The first concerns the fact that transmission suites almost always use acoustic linings on the heavyweight walls and floors of a transmission suite to suppress flanking transmission, but these were not considered. The second is that the ground floor damping can vary significantly between different laboratory designs and this has a significant effect on vibration transmission. The third is that their TSEA model did not include the back walls of the source and receiving rooms, although the effect of these walls on steady-state energy flow in building structures has been predicted to be significant [3]. The fourth concerns the potential for in-plane wave generation at junctions in the mid- and high-frequency range which were not included in the TSEA model. The fifth aspect concerns the fact that comparisons with impulse measurements on the Perspex scale model did not use backwards-integration for the excited plate. All of these aspects are considered in the measurements and predictions within this paper.

This paper uses TSEA to investigate structural decay curves for masonry/concrete walls and floors in both the laboratory and the field. The first stage is to validate the decay curves from the TSEA model against measurements on a large building formed by concrete/masonry walls and floors because (as far as the authors are aware) there are currently no such published validations in the literature. This model is then used in a series of numerical experiments to quantify the error in the estimate of the total loss factor when using different evaluation ranges to calculate the structural reverberation time. Numerical experiments are necessary for the following reasons: (a) to overcome the practical difficulties and expense that would occur in comparing different laboratory set-ups, (b) to avoid the effects of measurement uncertainty due to the spatial variation in vibration response over the plate surface, and (c) to give insight into the underlying reasons for the errors. The results from the modelling allow the identification of evaluation ranges which can be considered as being ideal for the measurement of the structural reverberation time. Optimal evaluation ranges are then identified for measurement protocols after considering the signal processing that adversely affects the initial part of the decay curve. To assess the error that can be considered tolerable in the total loss factor, Statistical Energy Analysis (SEA) is used to model different laboratory and field constructions. From these models it becomes apparent that other significant errors are incurred due to energy flow between the

test element and the other structural elements that form transmission suites, flanking laboratories or real buildings.

The intention is to reconcile the three main issues that have historically caused problems when measuring structural reverberation times on heavyweight walls and floors; these are (1) the evaluation range that is needed to ensure that the total loss factor calculated from the decay curve is representative of the true total loss factor, (2) the errors in the total loss factor when placed in the context of the other errors that occur due to energy flow between the test element and the connected structure, and (3) the signal processing that is necessary to measure and evaluate short decays.

2. Statistical Energy Analysis: Steady-state and transient models

This section describes the steady-state and transient forms of SEA used for the numerical experiments. In all cases, it is the resulting bending wave energy in subsystems that is of primary interest, where the power is only injected into bending wave subsystems. A bending wave only model is used for all one-third octave bands between 50Hz and 5kHz. In addition, a bending and in-plane wave model is used for one-third octave bands from 630Hz to 5kHz which corresponds to frequencies above the lowest fundamental in-plane mode on the walls/floors; each wall/floor is then represented by three subsystems that store modal energy for bending, transverse-shear and quasi-longitudinal waves. This approach is justified by previous work on heavyweight constructions by Hopkins [3].

2.1 Statistical Energy Analysis (SEA)

The use of steady-state SEA to predict sound transmission in buildings is an efficient and well-established approach due to the inherent uncertainty that exists in describing building structures [3,6]. Matrix SEA is used to determine the subsystem energies by accounting for all possible transmission paths using the following equation,

$$\begin{bmatrix} \sum_{n=1}^{N}\eta_{1n} & -\eta_{21} & \cdots & -\eta_{N1} \\ -\eta_{12} & \sum_{n=1}^{N}\eta_{2n} & & \\ \vdots & & \ddots & \\ -\eta_{1N} & & & \sum_{n=1}^{N}\eta_{Nn} \end{bmatrix} \begin{bmatrix} E_1 \\ E_2 \\ \vdots \\ E_N \end{bmatrix} = \begin{bmatrix} W_{\mathrm{in}(1)}/\omega \\ 0 \\ \vdots \\ 0 \end{bmatrix} \quad (1)$$

where η_{ij} is the Coupling Loss Factor (CLF) from subsystem *i* to *j*, and η_{ii} is the Internal Loss Factor (ILF) for subsystem *i* and $W_{\mathrm{in}(i)}$ is the power input into subsystem *i*.

Path analysis is used to determine sound transmission when power is injected into subsystem 1 and an energy level difference is required between subsystem 1 and subsystem *N* for transmission along a chain of subsystems, 1-2-3…*N*, where

$$\frac{E_1}{E_N} = \frac{\eta_2\eta_3 \ldots \eta_N}{\eta_{12}\eta_{23} \ldots \eta_{(N-1)N}} \quad (2)$$

where η_i is the Total Loss Factor (TLF) for subsystem *i*.

2.2 Transient Statistical Energy Analysis (TSEA)

TSEA makes use of the power balance equations in the time domain as described by Powell and Quartararo [7]. The loss factors used in steady-state SEA describe a physical behaviour that does not vary with time. However, it is reasonable to use steady-state SEA loss factors in TSEA, by ensuring that the time-interval is large enough to allow a reverberant field to form in each excited subsystem in each time step. Recent validations of TSEA by the authors using laboratory measurements have confirmed that the use of steady-state coupling loss factors is reasonable for both sound radiation [8] and structural coupling [9].

For a structure-borne sound power input into bending wave subsystem *i*, the energy at time, *t*, is $E_i(t)$. The change in energy is defined by the difference between the power gained and the power lost by that subsystem, hence

$$\frac{\mathrm{d}E_i(t)}{\mathrm{d}t} = W_{\mathrm{gain}(i)}(t) - W_{\mathrm{loss}(i)}(t) \quad (3)$$

which can be expanded for a system comprised of N subsystems as

$$\frac{\mathrm{d}E_i(t)}{\mathrm{d}t} = \left[W_{\mathrm{in}(i)}(t) + \sum_{j(j\neq i)}^{N} \omega\eta_{ji}E_j(t)\right] - \left[\omega\eta_{ii}E_i(t) + \sum_{i(i\neq j)}^{N} \omega\eta_{ij}E_i(t)\right] \tag{4}$$

where $E_i(t)$ is the time-varying energy in subsystem i, and $W_{\mathrm{in}(i)}(t)$ is the time-varying power input into bending wave subsystem i.

Equation (4) can now be re-written so that a finite difference method can be used to solve the energy balance. This allows a solution for the subsystem energy in the next time step, and by using the relationship between the internal, coupling and total loss factors, the "power loss" term can be simplified, giving

$$E_i(t_{n+1}) = E_i(t_n) + \Delta t\left[W_{\mathrm{in}(i)}(t_n) + \omega\left(\sum_{j(j\neq i)}^{N} \eta_{ji}E_j(t_n) - \eta_i E_i(t_n)\right)\right] \tag{5}$$

where $E_i(t_{n+1})$ is the energy at the next time step in subsystem i, $E_i(t_n)$ is the energy at the current time step in subsystem i, and Δt is the time interval.

An arbitrary value for the power is input into the source subsystem (i.e. the test element for which the structural decay for bending waves is to be evaluated) over a single time interval at t=0. At t=0 the energy in all subsystems is zero; hence the energy in each subsystem rises and then begins to decay as would the measured velocity level on a structure after transient excitation with a hammer hit. However, in a TSEA model there is no need to use backward-integration as there would be with measurements using impulse excitation.

When using steady-state loss factors it is necessary to ensure that the time interval, Δt, is large enough to allow a reverberant field to form in each excited subsystem during that time interval. In addition, the rate at which energy decays in the subsystem must be considered in order to avoid the decaying response being misrepresented in the time domain. The energy in a subsystem will decay exponentially according to $\exp(-\omega\eta\Delta t)$; hence considering the energy in a single subsystem, i, with power input at t_n=1, the ratio of energies in consecutive time steps is given by

$$\frac{E_i(t_{n+1})}{E_i(t_n)} = \exp(-\omega\eta\Delta t) \quad t_n \neq 1 \tag{6}$$

To achieve an accurate solution requires $\omega\eta\Delta t << 1$. For practical purposes, η corresponds to the largest TLF in each frequency band for the group of subsystems. As the TLF typically varies with frequency, the choice of time interval may also vary with frequency. The time interval for each frequency band must be sufficiently small such that it is defined by a constant, *b*, where

$$\Delta t \leq \frac{1}{b\omega\eta} \tag{7}$$

Before carrying out analysis with TSEA, it is necessary to prescribe the energy level difference between consecutive time steps to be –*C* dB, such that

$$10\lg\left[\frac{E_i(t_{n+1})}{E_i(t_n)}\right] = -C \text{ dB} \quad t_n \neq 1 \tag{8}$$

hence the constant, *b*, is calculated from

$$10\lg[\exp(-b^{-1})] = -C \text{ dB} \tag{9}$$

This approach allows the maximum change in the source subsystem energy level to be defined prior to evaluating the decay curves from the TSEA model. For coupled spaces and structures, energy will return to the source subsystem from other coupled subsystems; hence the exponential decay that occurs for a single subsystem will not occur in any decay comprising more than two consecutive time steps. Therefore the energy in the source subsystem will never decay faster than the rate determined by (9) because energy returning to this subsystem will always reduce the decay rate.

In this paper, the requirement is set at C=0.1dB which corresponds to $b\approx$43. This is significantly more stringent than b=3 which was proposed by Lyon and DeJong [10] but it has been found to be essential to ensure accurate representation of the early part of the decay.

The decay curves are evaluated over different ranges to give T_5, T_{10}, T_{15} etc. When measuring decay curves using sound pressure levels in rooms it is common to use forward filter analysis where the evaluation usually commences 5dB below the maximum level, partly to avoid significant signal processing errors [3]. As this is not relevant to the TSEA model for structure-borne sound, evaluation of the decay curve begins as soon as sufficient time has elapsed for bending waves to travel from an arbitrary excitation point on the source plate and undergo reflection from any of the plate boundaries,

then arrive at an arbitrary receiver point on the plate. On a statistical basis this distance is equal to the mean free path.

The structural reverberation time, $T_{s,X}$, is calculated using an evaluation range of XdB, from which the TLF is calculated using

$$\eta = \frac{6\ln 10}{2\pi f T_{s,X}} \tag{10}$$

3. Comparison of measured and TSEA predicted decay curves

The TSEA model is compared with structural decay measurements in a heavyweight building. This building forms a vertical transmission suite with suppressed flanking transmission (see Figure 1) that satisfies the International Standard ISO 10140. It contains a 140mm cast *in situ* concrete floor as a permanent test element for impact sound insulation measurements. The facility that houses the transmission suite and the transmission suite itself are modelled using two different TSEA models; a bending wave only model with 14 subsystems, and a bending and in-plane wave model with 38 subsystems that allows for the generation of bending and in-plane waves at each junction.

The subsystems represent the upper and lower rooms of the transmission suite, the 140mm concrete floor and the heavyweight walls/floors that are made from masonry or concrete. Internal loss factors for the rooms were calculated from measured reverberation times. The upper room of the transmission suite is formed from plasterboard walls which are not included in the model due to their significant impedance mismatch with the concrete floor and the fact that they are highly-damped. It is therefore reasonable to assume that they do not significantly affect energy flow in the system of heavyweight plates.

Material properties for the walls/floors were taken from measured data and are shown in Table 1. All coupling loss factors are calculated as described in Hopkins [3] using wave theory to determine the structural coupling and Leppington's theories for radiation efficiency with an adjustment at and above the critical frequency to limit the values to unity. This approach is justified by previous research using SEA with heavyweight constructions [3].

Structural decay measurements were taken using transient excitation from a plastic-headed hammer by processing the acceleration signal taken from an accelerometer. The signal processing used exponential averaging, backwards-integration and reverse-filter analysis whilst ensuring that BT>4 to prevent the one-third octave-band filters affecting the decay curve [11]. This is essential because decays on heavyweight walls/floors tend to be significantly faster than those in rooms. Measurements were taken at four different accelerometer positions for each of three excitation positions and an ensemble-average decay curve was calculated from the arithmetic average of the mean-square response at all these positions.

Measured and predicted decay curves for the 140mm concrete floor can be compared in Figure 2 for a range of one-third octave bands over the building acoustics frequency range. The individual and ensemble-average measured decays show distinct curvature which typically begins between the -5dB and -10dB down points. For this reason, only T_5 has been calculated by using an evaluation start point that is approximately 3dB down from the maximum level. Calculating $10\lg(T_{5,\mathrm{TSEA}}/T_{5,\mathrm{measured}})$ indicates that TSEA underestimates the measured T_5 by up to 3dB for the bending only model between 50Hz to 5kHz, up to 2dB for the bending only model between 630Hz to 5kHz and up to 4dB for the bending and in-plane model between 630Hz to 5kHz. Hence when determining T_5 in the high-frequency range (630Hz to 5kHz) where in-plane waves are generated, there is no clear improvement in accuracy by using a bending and in-plane model rather than a bending wave only model. Previous research [12] using SEA to predict the steady-state vibration response on masonry walls connected via L-junctions indicates that models considering only bending waves are usually sufficient over the building acoustics frequency range, but that bending and in-plane models are essential for T- and X-junctions. It is reasonable to assume that in-plane wave generation could be responsible for long secondary decays. However, there is no evidence that the bending and in-plane models provide better estimates of the secondary decay than the bending only model for this particular heavyweight building.

In the 125, 250 and 500Hz one-third octave bands, the predicted mode counts for a plate with simply supported boundaries are only 1.4, 2.9 and 5.7 respectively. From Figure 2 it is seen that it is only at 500Hz that there is generally good agreement between the measured and predicted decay

curves down to at least the -20dB down point. At 125Hz the TSEA model overestimates the late energy that returns to the source subsystem, causing longer secondary decays than are actually measured after the -20dB down point. This can be attributed to the wave theory used to calculate the structural coupling loss factors which tends to give slight overestimates for concrete/masonry walls/floors due to their low modal density and low modal overlap in the low-frequency range [3]. This trend is reversed at and above 2kHz where TSEA underestimates the energy returning to the source subsystem after the -15dB down point.

Figure 3 shows the difference between the measured and SEA predicted TLF that has been calculated using T_5. These differences are shown for the 140mm concrete floor and the four 215mm masonry walls that form the lower room. At most frequencies the 95% confidence intervals of the measured data overlap the 0dB line (i.e. no error) but there is a trend for the wave theory used in the models to overestimate the structural coupling, typically resulting in a few decibels difference between the TLFs.

4. Laboratory and field scenarios for building acoustics measurements

Numerical experiments with SEA and TSEA are now used to assess the errors in structural reverberation times and their influence on the measurement of sound insulation in transmission suites and junction transmission loss in flanking laboratories and in the field.

4.1 Transmission suites

In transmission suites, the structural reverberation time is useful when measuring airborne or impact sound insulation of test elements such as solid, heavyweight walls and floors in order to compare the results from different laboratories [1]. Figure 4 shows two idealized transmission suites for airborne sound insulation, Types A and B. These are both formed from 200mm cast *in situ* concrete plates (ρ_s=440kg/m^2, c_L=3800m/s, ν=0.2, η_{ii}=0.005). The plate that forms the test element represents a 100mm wall of lightweight aggregate masonry (ρ_s=140kg/m^2, c_L=2200m/s, ν=0.2, η_{ii}=0.01). All plates are modelled as being isotropic and homogenous with material properties taken from average measured values [3].

The Type A construction has physically disconnected rooms with the test element built on the source room side of the structure so that it forms L-junctions with the walls and floors that form the source room. In contrast, the Type B construction has physically connected rooms where the test element forms T-junctions with the walls and floors that form the source and receiving rooms.

Different realizations of the idealized transmission suites are considered in order to illustrate the effect of the laboratory on the structural decay curve of the test element when bending waves are mechanically excited. An important decision in the design of a transmission suite is whether the ground floor slabs should be 'earthed' or 'unearthed' (electrical analogy). An unearthed model is introduced which assumes that the TLF of the ground floor slabs equals the sum of the coupling loss factors plus the internal loss factor for *in situ* concrete. This would represent a laboratory with rooms mounted on vibration isolators to reduce background noise and flanking transmission between the source and receiving rooms. In the earthed model, the ground floor slabs have additional damping because the slabs are assumed to be in direct contact with the earth over their complete surface; this is simulated by setting the internal loss factor of each ground floor plate to $f^{-0.5}$ which is justified by measurements on actual ground floors [3]. It is assumed that there is no transmission of vibration between the two floor slabs via the earth; hence no coupling via ground-borne wave motion is considered in the model. A decoupled model is also introduced which assumes that the test element is physically decoupled from the structure but has the same TLF as if it were still connected. Whilst this particular situation is not physically realizable, it provides a useful benchmark from which to assess the effect of the ground floor slabs being 'earthed' or 'unearthed'.

For Types A and B the radiation coupling between the rooms and the plates that form the laboratory is set to zero to simulate a transmission suite with ideal (i.e. perfect) wall/floor linings. This prevents any excitation of these plates by the sound field and prevents any sound radiation from these plates into the rooms. In practice the closest physical realisation of these wall linings would be independent linings that are formed from thin plates with a high critical frequency such as plasterboard on an isolated frame. The use of such wall linings means that the results for Type A in this paper equally apply to a situation where (a) the test element is connected to the receiving room instead of the source room, or (b) the source and receiving rooms are swopped over, or (c) the test

element is fixed into the source room and the receiving room is a lightweight construction (e.g. plasterboard on a light metal frame).

The TLF of the test elements depends on how they are installed and connected to the laboratory structure; hence it is only the straightness or curvature of individual decay curves that can be compared because the TLF will differ in each situation. For comparative purposes, the tabulated percentage errors in the TLF are calculated from the TLF that is entered as input data in the TSEA model and T_5, T_{10}, T_{15} and T_{20} from the decay curve. In this paper, errors less than 10% in the TLF (linear) can be considered as negligible because this corresponds to only a 0.4dB error.

4.1.1 The effect of reverberant sound in the source and receiving rooms on the structural decay

An investigation is now made into the effect of the room reverberation times on the measured structural decay curve of the test element by structurally decoupling it from the Type A transmission suite. In this situation the TLF of the test element is equal to the sum of the internal loss factor and the radiation coupling loss factors, and because it is decoupled there is no generation of in-plane waves; hence the bending only model is used for all frequencies.

It is assumed that the source and receiving rooms have the same reverberation time as each other. Hence by varying the reverberation time of the rooms, it is possible to observe how the sound fields affect the structural decay on the test element. These room reverberation times are chosen to be 0.75, 1.5, 3 and 6 s. The decay curves and percentage errors are shown in Figure 5 for the 125, 250, 500 and 1k Hz one-third octave bands. The percentage error in the total loss factor, $e(\eta_{TX})$, determined using T_X is calculated using $e(\eta_{TX}) = (T_{X,\mathrm{TSEA}} - T_X) \,/\, T_X \times 100$ where $T_{X,\mathrm{TSEA}}$ is the structural reverberation time that is entered as input data into the TSEA model and T_X is the structural reverberation time determined from the decay curve that is output from the TSEA model. From Equation (10) this can be seen to be equivalent to $e(\eta_{TX}) = (\eta_X - \eta_{X,\mathrm{TSEA}}) \,/\, \eta_{X,\mathrm{TSEA}} \times 100$.

The results show that as the room reverberation time increases, more energy returns to the test element due to radiation coupling. This causes decays with a distinct double slope. However, above 1kHz the errors in the TLF are found to be negligible when using an evaluation range up to 20dB for the structural reverberation time. Fortunately, the double-sloped decays will rarely affect the ability to

accurately estimate the TLF even when there are long reverberation times (i.e. 6s) in the source and/or receiving rooms. This is because the secondary slope does not occur until the level has dropped by at least 15dB; hence there is sufficient dynamic range to evaluate the decay curve using T_5, T_{10} or T_{15} without the energy returning from the rooms significantly affecting the measurement. To assess the generality of this finding, TSEA models have also been run using (a) the same test element with a much higher TLF (i.e. as if it was rigidly connected to the laboratory structure) and (b) a 12.5mm plasterboard wall. These models result in the same conclusion, i.e. that errors are negligible when using T_5, T_{10} or T_{15} to measure the structural reverberation time as long as the room reverberation time is no longer than 6s.

4.1.2 Comparison of Type A and B transmission suites

Figures 6a and 6b allow comparison of the TSEA decay curves in one-third octave bands for the decoupled test element with the test element in Type A and B transmission suites. For this comparison the source and receiving room reverberation times are chosen to be 1.5s at all frequencies because International Standards [13] imply that values should generally be between 1 and 2s. This also ensures that the decay curve for the decoupled test element is unaffected by the room reverberation times over the first 30dB of the evaluation range as previously shown by Figure 5. Therefore over this evaluation range the model for the decoupled test element can be compared against the unearthed and earthed models of the Type A and B transmission suites. For Types A and B, the decay curves for the unearthed model are distinctly non-linear at all frequencies due to energy returning from the transmission suite walls and floors. For 1k, 2k and 4kHz the bending and in-plane model causes multiple-slope decay curves for both the unearthed and earthed situation due to a larger number of subsystems (representing quasi-longitudinal and transverse shear waves) that return energy to the test element. For the unearthed and earthed transmission suites at all frequencies, the percentage error in the TLF increases as the evaluation range increases due to non-linear decay curves. In general, the decay curves show greater curvature for the unearthed model compared to the earthed model.

Figure 7 shows the error in decibels for the TLF over the entire frequency range with Type A and B transmission suites when earthed and unearthed. This error is calculated using $10\lg(1+(T_{X,\mathrm{TSEA}} - T_X)/T_X)$ where $T_{X,\mathrm{TSEA}}$ is the structural reverberation time that is entered as input data into the TSEA

model and T_X is the structural reverberation time determined from the decay curve that is output from the TSEA model. Due to the multiple-slope decay curves, a smaller evaluation range for the structural reverberation time yields lower errors for the TLF. The errors are significantly lower when the transmission suites are earthed compared to when they are unearthed. Essentially the earthing is providing a 'sink' to dissipate energy in the ground; hence less energy is available to return to the test element. The results indicate that for earthed and unearthed laboratories (Type A or B) it is beneficial to evaluate the decay curve using T_5 to avoid significant errors.

In reality, transmission suites are often isolated from the ground using vibration isolators to reduce the background noise levels in the rooms and suppress flanking transmission; this corresponds to the unearthed situation. However, the TSEA models indicate that the unearthed situation gives larger errors in the TLF than the earthed situation; hence isolating the rooms in a transmission suite has potential disadvantages.

Figure 8a shows the predicted error in the sound reduction index, *R*, due to vibrational energy which is transmitted from the test element to the connected walls and floors of the laboratory, then transmitted back to the test element. This error is calculated by subtracting the sound reduction index that is predicted by matrix SEA (equation (1)) from the sound reduction index predicted using SEA path analysis (equation (2)) for direct transmission across the test element (resonant and non-resonant transmission). Figure 8a shows that vibrational energy flow involving the test element and the laboratory walls/floors (Type A or B) causes a small underestimate of the actual sound reduction index. Typically this error in the sound reduction index is less than 1dB over the building acoustics frequency range. This may be considered negligible in comparison with other measurement uncertainties.

The sound reduction index of a heavyweight wall or floor that is measured in a laboratory is of limited usefulness in acoustic design work without an accompanying measurement of the structural reverberation time. This additional measurement allows the following conversion of the measured sound reduction index from situation A in the laboratory, to situation B where the structural coupling losses are different, i.e. in a different laboratory or in the field.

$$R_{\mathrm{B}} = R_{\mathrm{A}} + 10\lg\left(\frac{\eta_{\mathrm{B}}}{\eta_{\mathrm{A}}}\right) = R_{\mathrm{A}} + 10\lg\left(\frac{T_{\mathrm{s(A)}}}{T_{\mathrm{s(B)}}}\right) \quad (11)$$

With this conversion it is now possible to calculate the error in the sound reduction index due to both energy flow around the laboratory structure using SEA models and the error incurred in determining the structural reverberation times from the decay curves using TSEA models. Figures 8b and 8c show this combined error when using structural reverberation times of T_5 and T_{20} respectively. Combining the errors causes the slight underestimate of the sound reduction index due to vibrational energy flow around the laboratory (Figure 8a) to be partly compensated by the error incurred using T_5 to determine the TLF (Figure 8b) but over-compensated by the error using T_{20} to determine the TLF (Figure 8c). Between 50Hz and 4kHz, using T_5 results in an error which is typically less than 1dB, but can be up to 4dB with T_{20}. This provides the motivation to try and measure structural reverberation times using T_5 wherever possible for heavyweight test elements in transmission suites.

4.2 Structural coupling measurements on junctions of heavyweight walls and floors

The most common types of structural coupling parameter that are required for junctions in the laboratory or the field are the coupling loss factor, η_{ij}, and the vibration reduction index, K_{ij}, between subsystems *i* and *j*. Both of these parameters require measurement of the structural reverberation time.

4.2.1 Laboratory measurements

In flanking laboratories where structural coupling is measured on junctions of connected heavyweight walls/floors the situation can be more complex than the transmission suite due to the number of transmission paths that determine the mean-square velocity on each plate that forms the junction. Arranging a test set-up to measure structural coupling parameters between heavyweight building elements is inherently awkward. Masonry/concrete elements are sufficiently heavy that they need structural support, and they ideally need to be connected to other parts of a building structure so that the TLFs of the elements are representative of *in situ* values. It is commonly assumed that a heavyweight laboratory structure can be defined so that it does not play a significant role in vibration transmission between heavyweight plates that form a junction; however it will be shown here that this is rarely the case.

Experimental SEA (ESEA) can be used to determine the coupling loss factors using either matrix ESEA or simplified ESEA [14]. Matrix ESEA typically requires measurement of the power input but this is not possible on many building elements because of the difficulty in fixing force transducers and impedance heads. Another problem is that the spatial variation of vibration over masonry/concrete walls or floors is quite high due to relatively low modal densities and physical imperfections. This can lead to errors in the subsystem energies that cause the matrix to be ill-conditioned. The result can be negative loss factors which are physically meaningless. In addition, when using matrix ESEA with more than two subsystems it is common for the matrix inversion to produce negative coupling loss factors; hence it is limited in its application to only L-junctions.

Simplified ESEA avoids errors with matrix inversion as it assumes that in the building system under study, the source and receiver subsystems simply form a two-subsystem SEA model. For this reason it is a practical approach in building acoustics. Simplified ESEA requires exciting subsystem *i* to measure the velocity level difference, $D_{v,ij}$, between subsystems *i* and *j*, so that the coupling loss factor is calculated using

$$\eta_{ij} = 10\lg(\eta_j) - \left(D_{\mathrm{v},ij} + 10\lg\left(\frac{m_i}{m_j}\right)\right) \tag{12}$$

where η_j is the TLF of subsystem *j* determined using equation (10) and m_i and m_j are the mass (kg) of subsystems *i* and *j* respectively.

Simplified ESEA has three requirements that must be met in order to ensure that the structural coupling can be determined. Requirement No.1 is that the TLF of the receiver subsystem needs to be sufficiently high that equipartition of modal energy does not occur. Requirement No.2 is that there must be negligible power flow back from receiving subsystem *j* to source subsystem *i*. Requirement No.3 is that any other connected subsystems must act as places of energy dissipation, not as conduits for significant flanking transmission between the source and receiver subsystems.

For homogeneous plates the vibration reduction index is related to the coupling loss factor according to [3]

$$K_{ij} = 10\lg\left(\frac{1}{\eta_{ij}}\right) + 5\lg\left(\frac{c_0^2 L_{ij}^2 f_{\mathrm{c},j}}{\pi^4 S_i^2 f_{\mathrm{c},i} f_{\mathrm{ref}} f}\right) \tag{13}$$

where L_{ij} is the junction length (m), S_i is the area of subsystem i and f_{ref} is a reference frequency of 1kHz. Note that for CLFs determined from wave theory assuming statistical modal densities, the value of K_{12} calculated from η_{12} will be the same as that calculated from η_{21}. However, in this section K_{ij} is calculated for each CLF separately and shown on the figures to illustrate the (relatively small) differences that occur when using simplified ESEA.

Using the same assumptions as simplified ESEA for two subsystems i and j, the measurement of the vibration reduction index is given in International Standards [4] as

$$K_{ij} = \frac{D_{\text{v},ij} + D_{\text{v},ji}}{2} + 10\lg\left(\frac{L_{ij}}{\sqrt{a_i a_j}}\right) \tag{14}$$

where the equivalent absorption length, a, for subsystem i is calculated from the structural reverberation time using

$$a_i = \frac{2.2\pi^2 S_i}{c_0 T_{\text{s}(i)}}\sqrt{\frac{f_{\text{ref}}}{f}} \tag{15}$$

To assess the laboratory situation, the following example is chosen; a T-junction of heavyweight walls comprising a 215mm separating wall (430kg/m^2) and two 100mm flanking walls (200kg/m^2), these are all made from dense aggregate masonry. The concrete floors on which each walls rests are made from 150mm concrete (330kg/m^2). The material properties are [3]: ρ =2200kg/m^3, c_{L}=3800m/s, ν=0.2, η_{ii}=0.005 for concrete, and ρ =2000kg/m^3, c_{L}=3200m/s, ν=0.2, η_{ii}=0.01 for dense aggregate masonry.

A flanking laboratory is defined by any space and/or structure into which a test junction can be built; hence a sequence of four idealised test arrangements is now considered to gain insight into the practical issues. These different test arrangements are shown in Figure 9. For flanking laboratories an important factor is whether the ground floor slab is ‘earthed’ or ‘unearthed’ (defined in Section 4.1) because an ‘earthed’ slab provides a sink for vibrational energy. To assess the effect of the laboratory structure it is initially useful to consider the test junction in isolation. This is arrangement A where the junction is completely isolated from any other structure and essentially represents a situation where the test junction is resiliently suspended in space. Although this is extremely difficult

to arrange in practice, it does corresponds to a practical situation where the aim is to reduce flanking transmission by building each wall in the junction on top of strips of resilient material which have a very low dynamic stiffness. Arrangement B considers the same isolated junction but where each plate in the test junction has been given the same TLF as if it were built to form two rooms that form a flanking laboratory. Note that for heavyweight walls and floors this can rarely be realized in practice; however one can consider a similar situation for laboratory measurements on junctions of thin metal plates where surface treatments are applied to the plates to achieve damping that is indicative of *in situ*. For each of the two rooms the floor and ceiling slabs are made from 150mm concrete (330kg/m^2), the two opposite walls are made of 215mm dense aggregate masonry (430kg/m^2) and the other two opposite walls are made of 100mm dense aggregate masonry (200kg/m^2). All walls and floors are assumed to be homogeneous isotropic plates. Arrangement C is a practical realization of a flanking laboratory where the junction is rigidly connected to a single, earthed ground floor. Arrangement D is another practical realization and consists of three individual, earthed ground floors to try and suppress unwanted flanking transmission compared to arrangement C.

Figures 10a and 10b show the decay curves from the TSEA model for wall 1 (separating wall) and wall 2 (flanking wall). The resulting errors in the TLF in decibels when calculated from T_5, T_{10}, T_{15} and T_{20} are shown on Figure 11.

For wall 1 (separating wall) in arrangements A, C and D, it is shown that reducing the evaluation range tends to reduce the error from the multiple-slope decay curves caused by energy returning to the source subsystem. Arrangements A and B represent isolated junctions where the walls have significantly different TLFs. For arrangement A the errors are only negligible for T_5; but significant curvature in the structural decays shows that isolating the test junction causes significant errors in accurately quantifying the TLF from structural decays when the evaluation range is larger than 10dB. With arrangement B each plate in the isolated test junction has the TLF it would have if it were connected to form two adjacent rooms. This results in negligible errors. In this sense it represents an ideal situation for an isolated junction, albeit one that will be difficult, or impossible, to realise in practice with heavyweight walls/floors. Arrangements C and D use highly-damped ground floors to support the plates and both arrangements give rise to significant errors. There is no clear

advantage in using disconnected ground floors (D) compared to a single, large ground floor (C). For the bending only model, significant errors can be avoided by using T_5. The bending and in-plane model (1k, 2k and 4k Hz) produces multiple-slope decay curves due to more subsystems returning energy to the separating wall, although this effect is less prominent with arrangement A and negligible for arrangement B.

For wall 2 (flanking wall) in test arrangements A, C and D, a smaller evaluation range also results in a smaller error. Comparing test arrangements C and D to A at and above 500Hz indicates that the use of highly-damped ground floors to support the walls results in larger errors. For arrangements A, C and D, the errors for wall 2 are lower than wall 1.This is noteworthy because it indicates that the error can be expected to vary significantly for different walls/floors that form a test junction.

The next stage is to quantify the error when using simplified ESEA to determine the CLF or K_{ij} in the laboratory or *in situ*. This includes the error in the TLF along with any error due to a failure to fulfil any of the three requirements of simplified ESEA due to the influence of the physical test set-up. Three different values are used for the TLF: (1) the exact value is used in equation (12) hence there is no error in the TLF, (2) the TLF is calculated using T_5 from TSEA and (3) the TLF is calculated using T_{20} from TSEA.

In the laboratory situation, Figure 12 shows the errors in η_{ij} and K_{ij} for arrangements C and D. Note that both these arrangements can be realised in practice. The results indicate that the errors with the former arrangement tend to be larger than with the latter. When considering only bending waves the errors are largest for transmission across the straight section of the T-junction from plate 2B to 3B where 'B' indicates that it is the bending wave subsystem for the plates that is being considered in both SEA models. The reason for this is that plate 1B and the concrete floors of the laboratory play a significant role in vibration transmission between plates 2B and 3B. Hence requirement No.3 for simplified ESEA is not satisfied. With the exact TLF it is seen that simplified ESEA overestimates η_{ij} (or underestimates K_{ij}). When T_5 is used to determine the TLF then the error in η_{ij} and K_{ij} is reduced slightly because the TLF is slightly underestimated. However, when T_{20} is used to determine the TLF,

this TLF is significantly underestimated such that the error in η_{ij} and K_{ij} tends towards 0dB. Hence simplified ESEA with T_{20} appears to give the right answer, but for the wrong reasons; namely the cancellation of two errors. The bending and in-plane model has stronger coupling between plates 2B and 3B than the bending only model; hence at high frequencies the error for transmission across the straight section is significantly lower than around the corner. However, the same problem occurs when T_{20} is used to calculate the TLF. These problems are in addition to the fact that modal overlap factors on free-standing junctions of heavyweight walls are lower than *in situ*; the implication of this is that structural coupling parameters will not be situation invariant [15].

4.2.2 Field measurements

In the field situation, T- and X-junction measurements are considered in a large building comprised of 27 rooms where each room is formed from the same walls and floors that were defined for Arrangement B. The T- and X-junctions are on the middle floor of the building as shown in Figure 13.

Figure 14 shows the errors in η_{ij} and K_{ij} for the T-junction as well as for an X-junction formed by the same types of walls. When the exact TLF is used, the errors are found to be similar or larger than when the junction is installed in a flanking laboratory. This is because requirement No.3 for simplified ESEA is not satisfied due to the many flanking paths in the building that transmit vibration between the source and receiver plates. The largest errors occur for transmission across the straight section of both the T- and X-junctions. As with the flanking laboratory, the same problem occurs when long evaluation times are used to determine the structural reverberation time, such as T_{20}, because the underestimate in the TLF tends to compensate for the overestimate of the receiver energy due to unwanted flanking transmission.

5. Evaluation procedure for structural decay curves

The structural decay curves from measurements and TSEA confirm that energy returns to the test element from the connected structure or coupled space. This can cause significant errors when estimating the TLF from the structural reverberation time depending on the choice of evaluation

range. It is concluded from previous sections in this paper that errors can be minimised by measuring T_5. Hence in this section, an evaluation procedure for the structural reverberation time, $T_{s,X}$, is proposed to overcome two connected issues relating to such a requirement: namely, the need for an evaluation start point to sometimes begin less than 5dB below the maximum level, and how to determine when it is appropriate to use evaluation ranges larger than X=5dB.

Not all structural decay curves will be significantly affected by energy returning to the test element. For this reason the evaluation procedure needs to identify when a decay curve is significantly affected by returning energy. The aim is to evaluate only the first slope of any multiple-slope decay curve whilst using the longest possible evaluation range to ensure that errors in determining the gradient are minimised. However, evaluation can only begin at the point where the filters and the detector do not distort the decay curve. Structural decays on heavyweight walls and floors are usually quite fast and one-third octave-band measurements are often required; hence it is advisable to always use reverse-filter analysis such that when BT>4 [11] the effect of the filter on the early part of the decay curve is negligible. Impulse excitation is beneficial because the necessary backwards-integration provides a smooth curve on which to identify the evaluation starting point and the evaluation range.

When measuring decay curves for sound pressure levels in rooms, the evaluation start point is usually 5dB below the maximum level. This avoids distortion of the decay curve from the filters and the linear or exponential averaging device and also excludes the time interval before the arrival of the first reflected wave in typical room volumes [3]. For structural decays a similar assessment is now made to determine whether the evaluation of T_5 could commence using an evaluation start point less than 5dB. If this were possible, it would beneficially extend the available evaluation range. This is assessed by processing exponentially-decaying sinusoids with reverse-filter analysis, backwards integration and both linear and exponential detectors. The detector distorts the true decay by introducing curvature in the early part of the decay. The size of the error partly depends on whether the detector is a linear or exponential averaging device and its respective time constant or averaging time. For room acoustics measurements, the International Standard ISO 3382-1 [16] requires the time constant of an exponential averaging device to be less than, but as close as possible to, T/30, and the

averaging time of a linear averaging device to be less than $T/12$. It also notes that for an exponential averaging device there is little advantage in setting the averaging time very much less than $T/30$, and for a linear averaging device there is no advantage in setting the interval between points at very much less than $T/12$. In the following analysis it is assumed that the fastest detectors in modern analysers intended for room acoustics applications typically have a time constant for exponential averaging of $\tau=1/1024$ and an averaging time for linear averaging of 1ms. These detectors are compared with those based on the limiting values described in ISO 3382-1. Processing the resulting decay curves allows calculation of the error in the TLF from structural reverberation times that are evaluated at start points between one and five decibels down from the maximum level.

An error in the TLF is calculated using $10\lg(1+(T_{\text{actual}} - T_5) / T_5)$ where T_{actual} is the actual (i.e. true) structural reverberation time and T_5 is the structural reverberation time determined from the decay curve that results from the signal processing. This error in the TLF is shown in Figure 15. A maximum error of -0.5dB in the TLF can be considered to be acceptable; hence this is drawn on the figure as a straight line (Note that this corresponds to a percentage error in the structural reverberation time of 12.2%). One of the advantages of exponential averaging using a frequency-dependent, fixed fraction of the reverberation time (i.e. $\tau=T/30$) is that the error is a function of the evaluation start point and is the same for all frequencies. This error in the TLF is always negative (i.e. underestimating the true value) but becomes negligible as the evaluation start point is changed from 0dB to -5dB. In contrast, the errors for linear averaging tend to fluctuate. However, linear averaging with an averaging time of 1ms gives significantly smaller errors than exponential averaging for the two time constants considered here. For practical purposes, either linear or exponential averaging can be used provided that a suitable averaging time or time constant is selected. In the future it would be beneficial if frequency-dependent detector times were implemented in state-of-the-art analysers that are intended for building acoustics measurements. For example, detector times could be based on a user-defined maximum total loss factor for heavyweight walls/floors when connected on all sides to other walls and floors. To ensure errors in the TLF are less than 0.5dB between 50 and 500Hz, the results indicate that when $BT>4$ the evaluation start point should be at least 2dB below the maximum level.

The next aspect to consider is that evaluation of the decay curve can only begin after the first reflected wave from the plate boundary arrives at the accelerometer. This requires knowledge of the distance from any excitation point (source) to any accelerometer position (receiver) in the central area of the plate where the vibration field is sampled. A Monte-Carlo simulation using geometrical ray-tracing is now used to calculate the probability distribution for source-to-boundary-to-receiver distances on a plate with a point source at many different locations. The distances in the probability distribution are normalised to the analytical solution for the mean free path, d_{mfp}. This represents the average boundary-to-boundary distance travelled by a wave in a diffuse field on a two-dimensional subsystem such as a plate and is given by

$$d_{\mathrm{mfp}} = \frac{\pi S}{U} \tag{16}$$

where S is the plate area and U is the plate perimeter.

Figure 16 shows the distribution of source-boundary-receiver distances, d_{sbr}, for a rectangular wall or floor (10 m^2) with excitation by a point source at random positions. Two different types of reflection are considered from the boundaries, diffuse or specular reflections. A central area on the plate for the receiver position (i.e. the accelerometer) is defined by a minimum distance of 0.5 m from the boundaries. This area is also used to choose random positions for the point source as well as to measure the decaying vibration field with the accelerometer. The mean value for d_{sbr} from the Monte-Carlo simulation is approximately equal to d_{mfp}. Hence d_{mfp} is used to represent the minimum distance from any excitation point to any accelerometer position in the central area of the plate although it should be noted that d_{sbr} goes as low as $0.5d_{\mathrm{mfp}}$.

Typical masonry/concrete walls can be assumed to have surface areas between 5 and 15m^2, thicknesses between 0.1 and 0.3m, and quasi-longitudinal wavespeeds between 1900 and 3800m/s whereas concrete floors typically have surface areas between 5 and 25m^2, thicknesses between 0.15 and 0.3m, and a quasi-longitudinal wavespeed of 3800m/s [3]. To calculate the time taken to travel the mean free path requires knowledge of the group speed and this is calculated assuming (a) thin plate bending wave theory over the entire frequency range as well as (b) thick plate theory above the

thin plate limit [3]. For masonry/concrete walls and floors it is reasonable to assume that the TLF is described by the equation, $Af^{-0.5}+\eta_{ii}$ where $0.3 \leq A \leq 1$ gives a reasonable indication of the range in the laboratory and the field [3]. Assuming that A=1 and η_{ii}=0.01 are indicative of the highest TLF that can be commonly found in heavyweight buildings [3,6], the time interval for the first reflection to be registered by the accelerometer will fall within the period before the 3dB evaluation start point, but only below 500Hz. Therefore it is proposed to revert to a 5dB evaluation start point above 500Hz.

In conclusion, it is proposed that reverberation times of masonry/concrete walls and floors could be measured with less than 0.5dB error in the TLF by using a starting point for the evaluation that is 3dB below the maximum level, an evaluation range of at least 5dB, and measuring with impulse excitation, backwards-integration and reverse-filter analysis whilst ensuring that BT>4.

The proposed procedure to evaluate the decay curve is summarized in Figure 17. Firstly, T_5 is calculated using a starting point that is ZdB below the maximum level. From the above analysis on masonry/concrete walls and floors, Z=3dB can be used for 50 to 500Hz and Z=5dB for 630Hz to 5kHz. The line of best-fit over an evaluation range larger than 5dB is then checked for similarity to the line of best-fit for the T_5 evaluation. This is done to detect curvature or multiple-slopes in the decay curve. If the two lines of best-fit are similar then the larger evaluation range can be considered to cover the same initial slope. If they are dissimilar, this indicates that the larger evaluation range extends over a secondary slope. Two stages are used to determine similarity between the two lines of best-fit. The first stage considers whether the gradient of the line of best-fit from the larger evaluation range falls within the confidence limits of the gradient of the line of best-fit from the T_5 evaluation. This uses the gradient [17] and the standard error of the gradient of the least-squares line of best-fit [18] to calculate the lower and upper confidence limits of plus or minus one standard deviation (≈68%) of the gradient [19]. The second stage determines when the error in the TLF is ±0.5dB, as calculated from the structural reverberation times using the line of best-fit from the larger evaluation range, Y, and the line of best-fit from the T_5 evaluation. For exponentially-decaying sinusoids it was previously seen on Figure 15 that all the TLF errors were <0dB. However, measured decay curves are not smooth and tend to fluctuate due to low modal density; hence the requirement is set as ±0.5dB.

Experience in using this procedure to process measurements from heavyweight walls and floors shows that the evaluation range for the initial slope typically varies between 5 to 25dB over the building acoustics frequency range. This indicates that it is rarely appropriate to use a single evaluation range to process all structural decay curves.

6. **Conclusions**

Structural decay curves predicted using TSEA for bending waves on heavyweight walls and floors are characterised by a short, fast, straight decay which is followed by distinct curvature due to energy returning from other parts of the building structure. This is confirmed by comparison of the TSEA model with measurements in a heavyweight building. For this reason, evaluation of the decay curve to determine the structural reverberation time can only occur over the initial part of the decay curve. The measurements indicate that when determining T_5 in the high-frequency range where in-plane waves are generated there is no clear improvement in accuracy by using a bending and in-plane wave model instead of a bending wave only model.

Numerical experiments simulating transmission suites demonstrate that the structural reverberation time of a heavyweight test element which is isolated from the laboratory structure tends to have a decay curve that is unaffected by the reverberant sound field in the source and/or receiving room over the first 15dB of the evaluation range. For this reason it is only appropriate to consider use of T_5, T_{10} or T_{15}. However, when a test element is rigidly connected to the heavyweight structure of the transmission suite there are multiple-slope decay curves due to energy returning to the test element from the laboratory structure. This causes significant errors in the TLF. For rigidly connected test elements, the errors in the TLF are lower when the source and receiving rooms have floors built directly onto the earth (which acts as a 'sink' to dissipate energy) compared to source and receiving rooms which are isolated from the ground, for example with vibration isolators. For most transmission suite designs it is concluded that it will be beneficial to evaluate the decay curve using T_5 to avoid significant errors.

Numerical experiments simulating structural coupling measurements on plate junctions in flanking laboratories show distinct curvature in the structural decays on masonry walls that form free-

standing junctions. These occur regardless of whether the walls are isolated by dynamically-soft resilient layers from the laboratory structure, or rigidly connected to highly-damped ground floors. This makes it a necessity to use T_5 to calculate the TLF. However, significant errors still occur when simplified ESEA is used to determine coupling loss factors or vibration reduction indices due to unwanted flanking paths that transmit vibration between the source and receiver plates. It is found that the use of simplified ESEA with TLFs determined from structural reverberation times with large evaluation ranges, such as T_{20}, can appear to give the right answer for the structural coupling parameter, but for the wrong reasons. This is due to the cancellation of two errors; the error in the TLF and the error due to unwanted flanking transmission.

The main finding is that for heavyweight walls and floors the errors in the calculated TLF can be minimised using T_5. However, in many cases this will require the evaluation start point to be less than 5dB below the maximum level. An evaluation start point of 3dB below the maximum level is feasible for the low- and mid-frequency ranges based on consideration of the signal processing errors in the early part of the decay and the fact that evaluation of the decay curve can only begin after the first reflected wave from the plate boundary arrives at the accelerometer. Another consideration is that not all structural decay curves will be significantly affected by energy returning to the test element. Hence an evaluation range greater than 5dB will sometimes be appropriate. For this reason an evaluation procedure is proposed which identifies when a structural decay curve is and is not significantly affected by energy returning to the test element such that, where appropriate, it is possible to use T_{10}, T_{15} etc.

Acknowledgements

The authors would like to thank Gary Timmins at the Building Research Establishment (BRE) for access to the vertical transmission suite to carry out the decay measurements. Matthew Robinson gratefully acknowledges the funding provided by a DTA grant from the Engineering and Physical Sciences Research Council and the University of Liverpool.

Table 1. Material properties for the transmission suite complex with a 140mm concrete separating floor.

Subsystem	L_x (m)	L_y (m)	L_z/h (m)	ρ_s (kg/m^2)	c_L (m/s^2)	η_{ii} (-)
Room 1	3.61	4.18	3.51	-	-	-
Room 2	3.33	3.92	3.91	-	-	-
Floor 3	4.19	3.61	0.14	345.4	3856	0.005
Wall 4	3.61	3.91	0.215	430	3200	0.01
Wall 5	4.19	3.91	0.215	430	3200	0.01
Wall 6	3.61	3.91	0.215	430	3200	0.01
Wall 7	4.19	3.91	0.215	430	3200	0.01
Floor 8	4.19	3.61	0.3	660	3680	0.005
Floor 9	14.03	9.15	0.3	660	3680	Measured
Wall 10	9.76	9.15	0.2	440	3680	0.005
Wall 11	14.03	9.76	0.2	1088	3680	0.005
Wall 12	9.76	9.15	0.2	440	3680	0.005
Wall 13	14.03	9.76	0.2	440	3680	0.005
Floor 14	14.03	9.15	0.2	440	3680	0.005

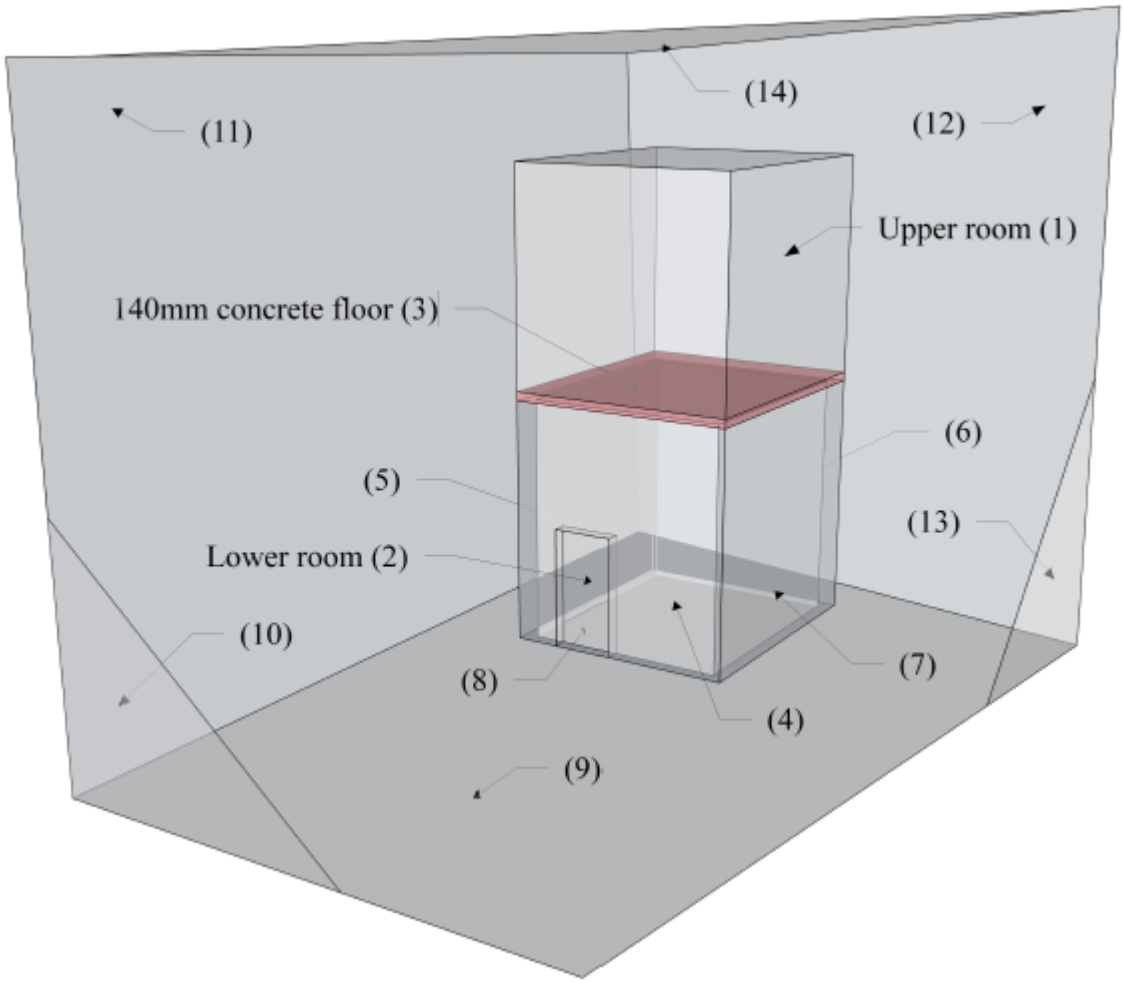

Figure 1. Vertical transmission suite complex with a 140mm concrete separating floor. The numbers in brackets indicate the 14 subsystems in the bending wave only TSEA model.

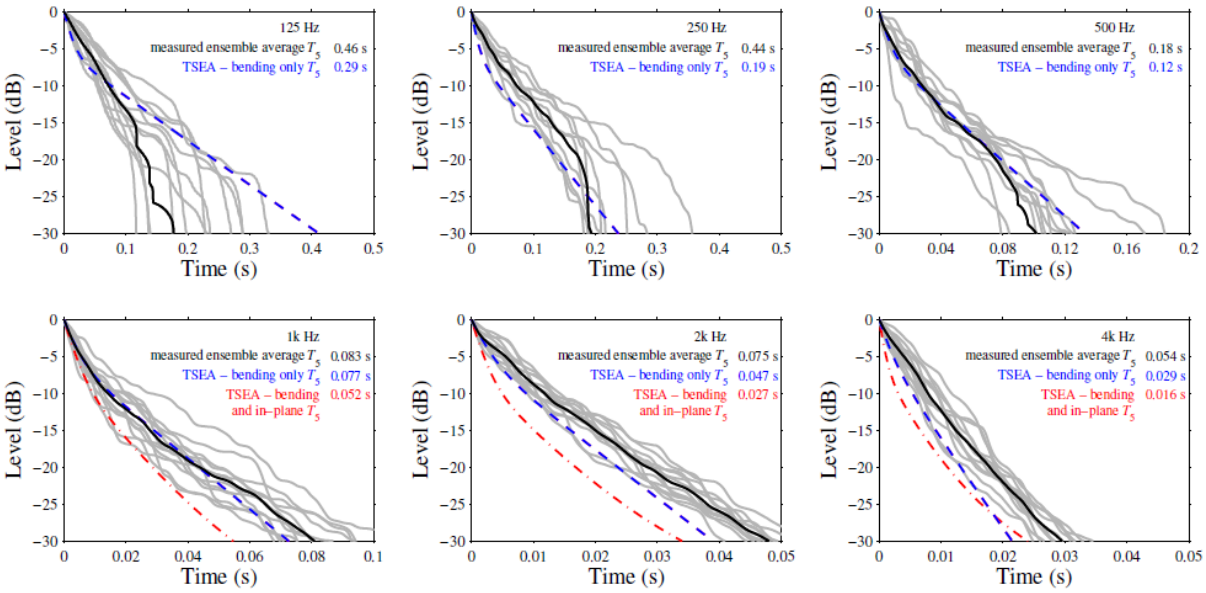

Figure 2. Comparison of measured and predicted decay curves for the 140mm concrete floor. Solid black curve represents the measured ensemble average. Dashed blue curve represents the bending only model, dash-dot red curve represents the bending and in-plane model, grey curves represent the individual measured decay curves from different positions on the floor.

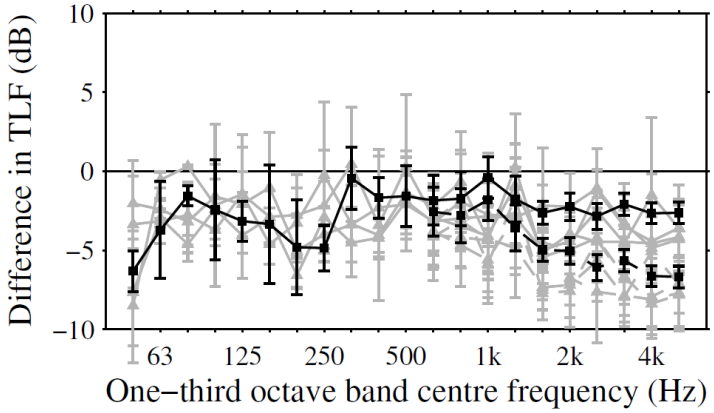

Figure 3. Difference between the total loss factors (measured minus SEA) for bending wave subsystems calculated using T_5. The black curve represents the 140mm concrete floor with the grey curves representing the four 215mm masonry walls that form the lower room. Solid lines represent the bending only SEA model (50Hz to 5kHz) and dashed lines represent the bending and in-plane SEA model (630Hz to 5kHz).

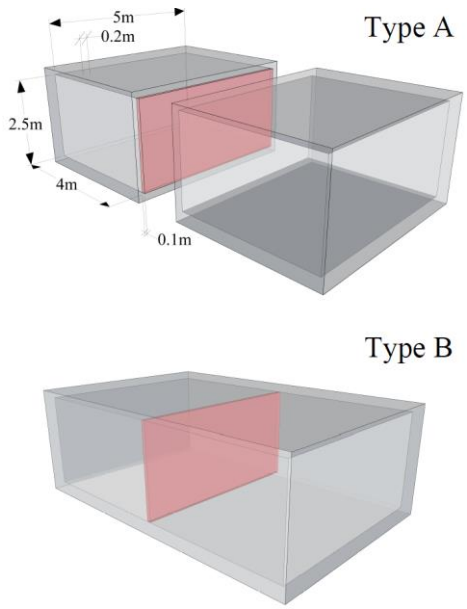

Figure 4. Idealized transmission suites (Types A and B) with the test element (100mm masonry wall) shown in red.

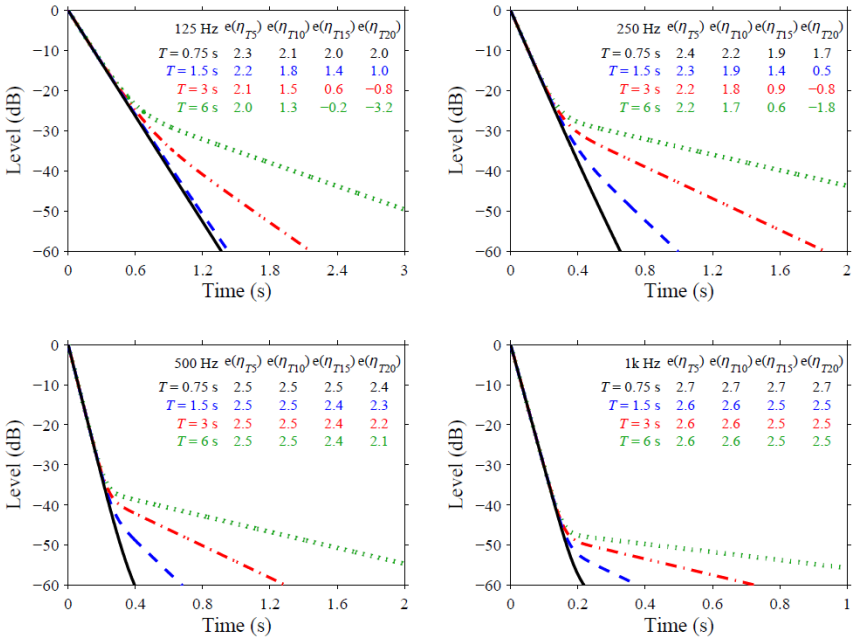

Figure 5. Predicted structural decay curves of the 100mm masonry wall when structurally decoupled from the Type A transmission suite to show the effect of the following source and receiving room reverberation times: 0.75s (solid black line), 1.5s (dashed blue line), 3s (dash-dot red line), 6s (dotted green line). Tabulated error e(η_{TX}) gives the percentage error in the total loss factor when calculated from the structural reverberation time with evaluation range, *X* dB.

a)

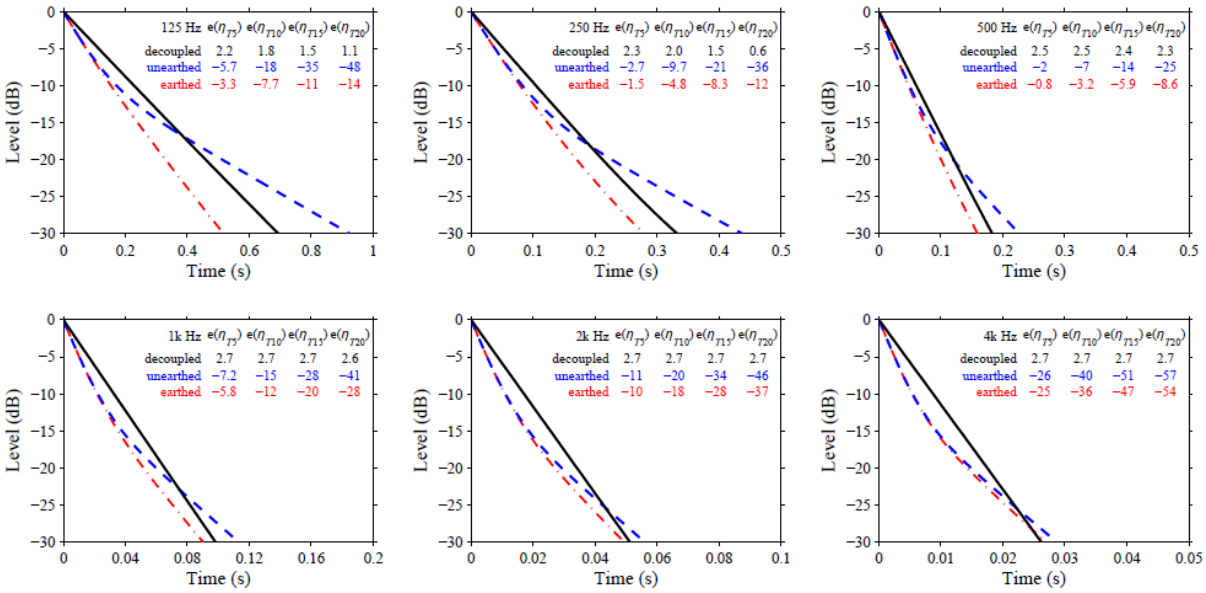

b)

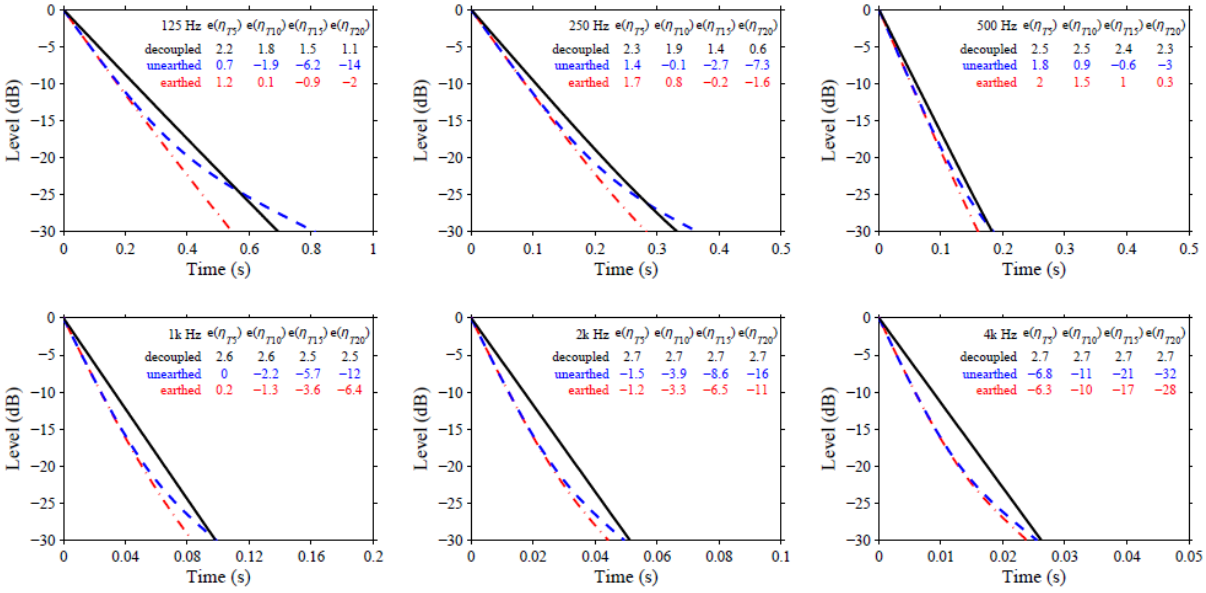

Figure 6. Structural decay curves for the 100mm masonry wall when rigidly connected to (a) Type A and (b) Type B transmission suites. The solid black line represents the decoupled test element, dashed blue line represents the unearthed ground floor, dash-dot red line represents the earthed ground floor. Tabulated error e(η_{TX}) gives the percentage error in the total loss factor when calculated from the structural reverberation time with evaluation range, *X* dB.

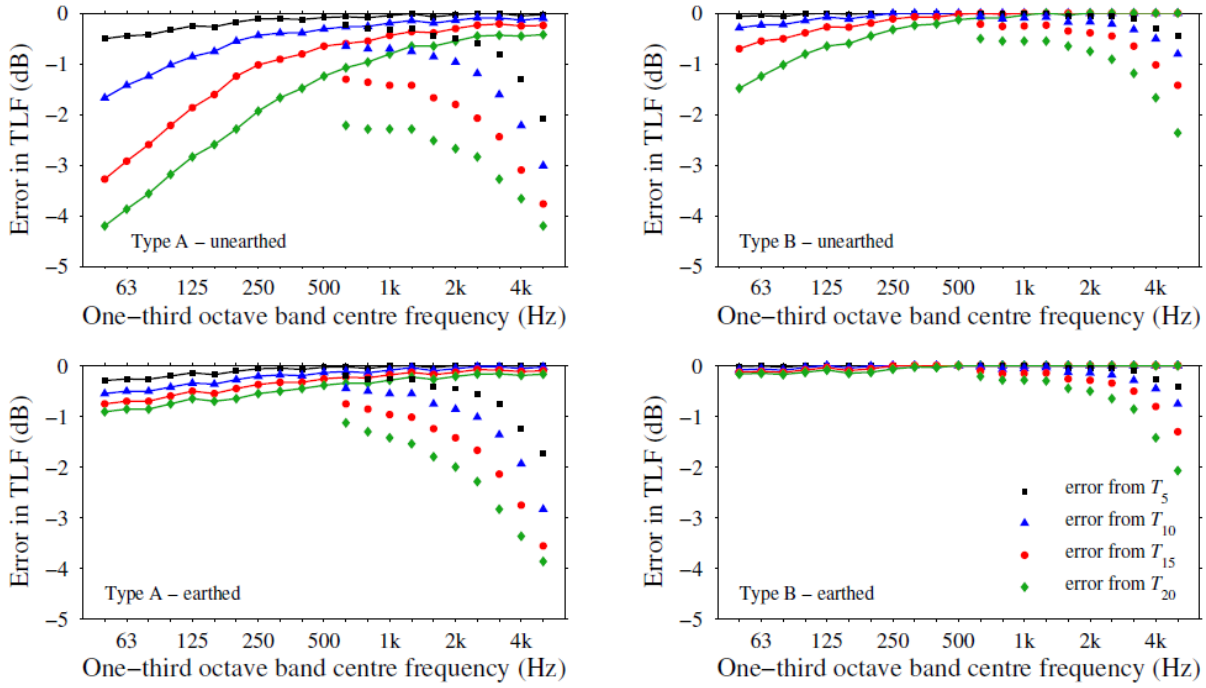

Figure 7. Errors in the total loss factor calculated using structural reverberation times with different evaluation ranges for the 100mm masonry wall installed in Type A and B transmission suites. Markers connected with solid lines represent the bending only model (50Hz to 5kHz). Markers without lines represent the bending and in-plane model (630Hz to 5kHz).

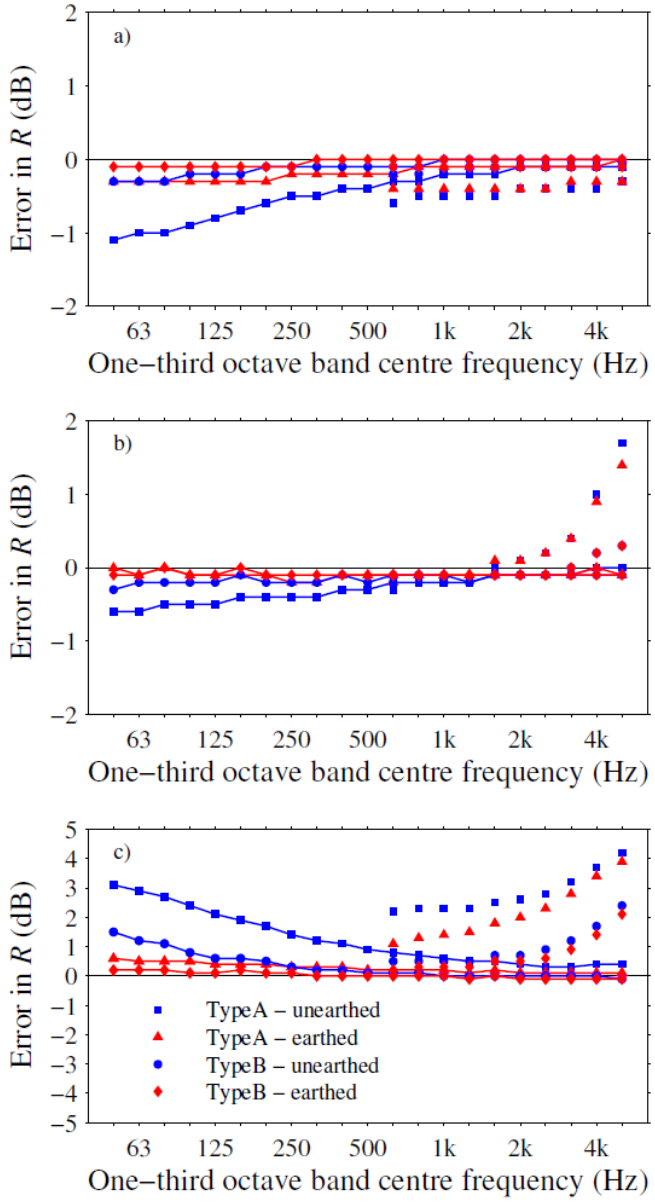

Figure 8. Error in the measurement of the sound reduction index for a 100mm masonry wall due to (a) energy flow between the wall and the laboratory structure, (b) the combination of energy flow and normalization using T_5, and (c) the combination of energy flow and normalization using T_{20}. Markers connected with solid lines represent the bending only model (50Hz to 5kHz). Markers without lines represent the bending and in-plane model (630Hz to 5kHz).

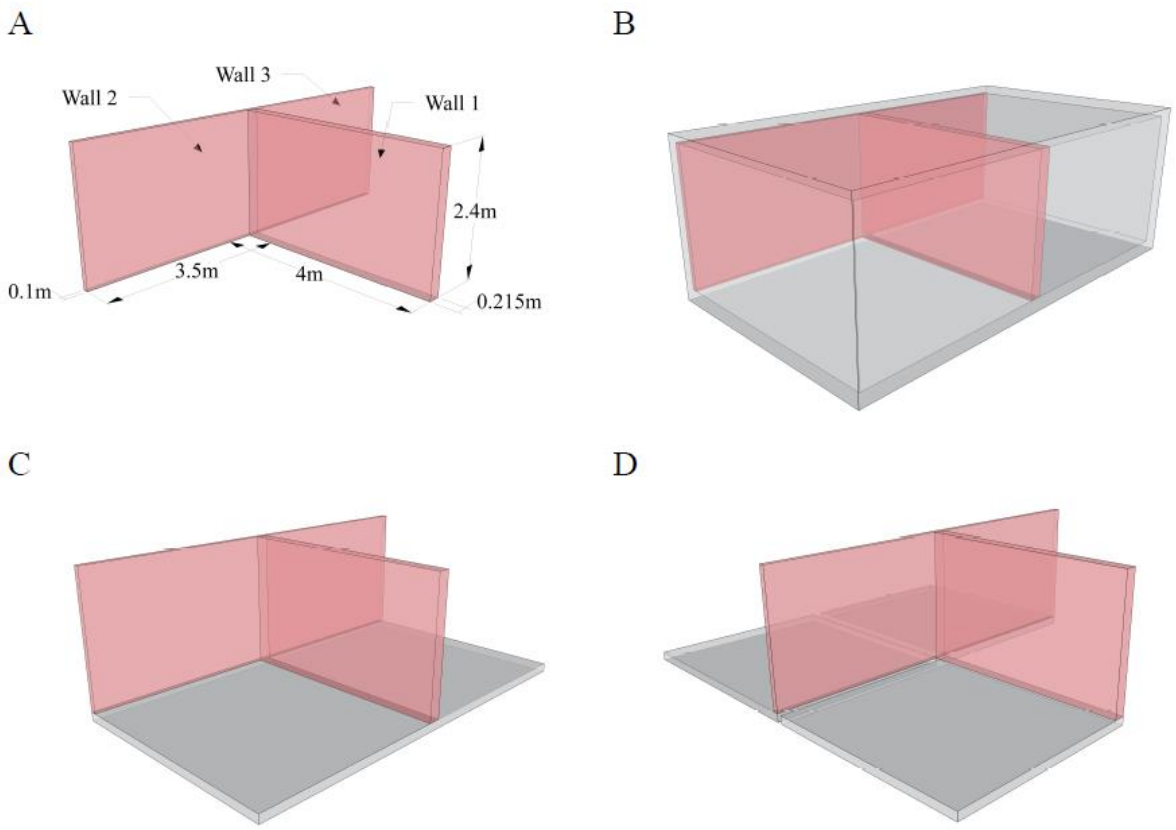

Figure 9. T-junction in four different test arrangements: A – isolated, B – isolated as in A but with modified total loss factors to simulate mounting in a flanking laboratory forming two rooms, C – all walls connected to a single ground floor, D – each wall connected to an individual ground floor. The walls that form the T-junction are shown in red.

a)

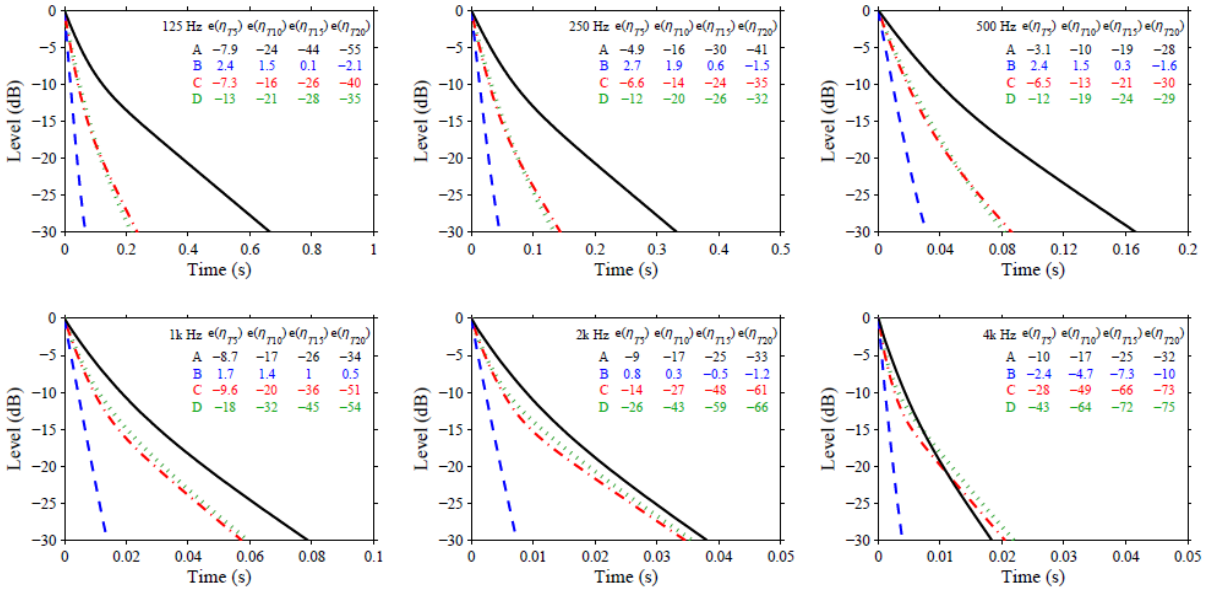

b)

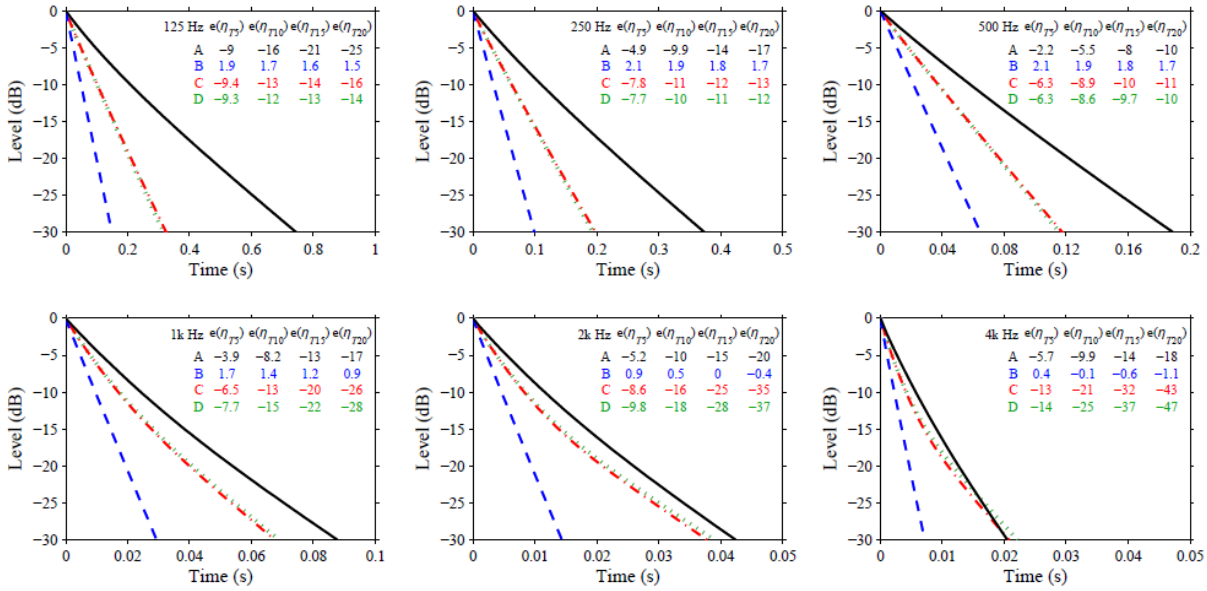

Figure 10. Structural decay curves for (a) Wall 1 and (b) Wall 2 from the T-junction in test arrangements A, B, C and D. Tabulated error e(η_{TX}) gives the percentage error in the total loss factor when calculated from the structural reverberation time with evaluation range, *X* dB.

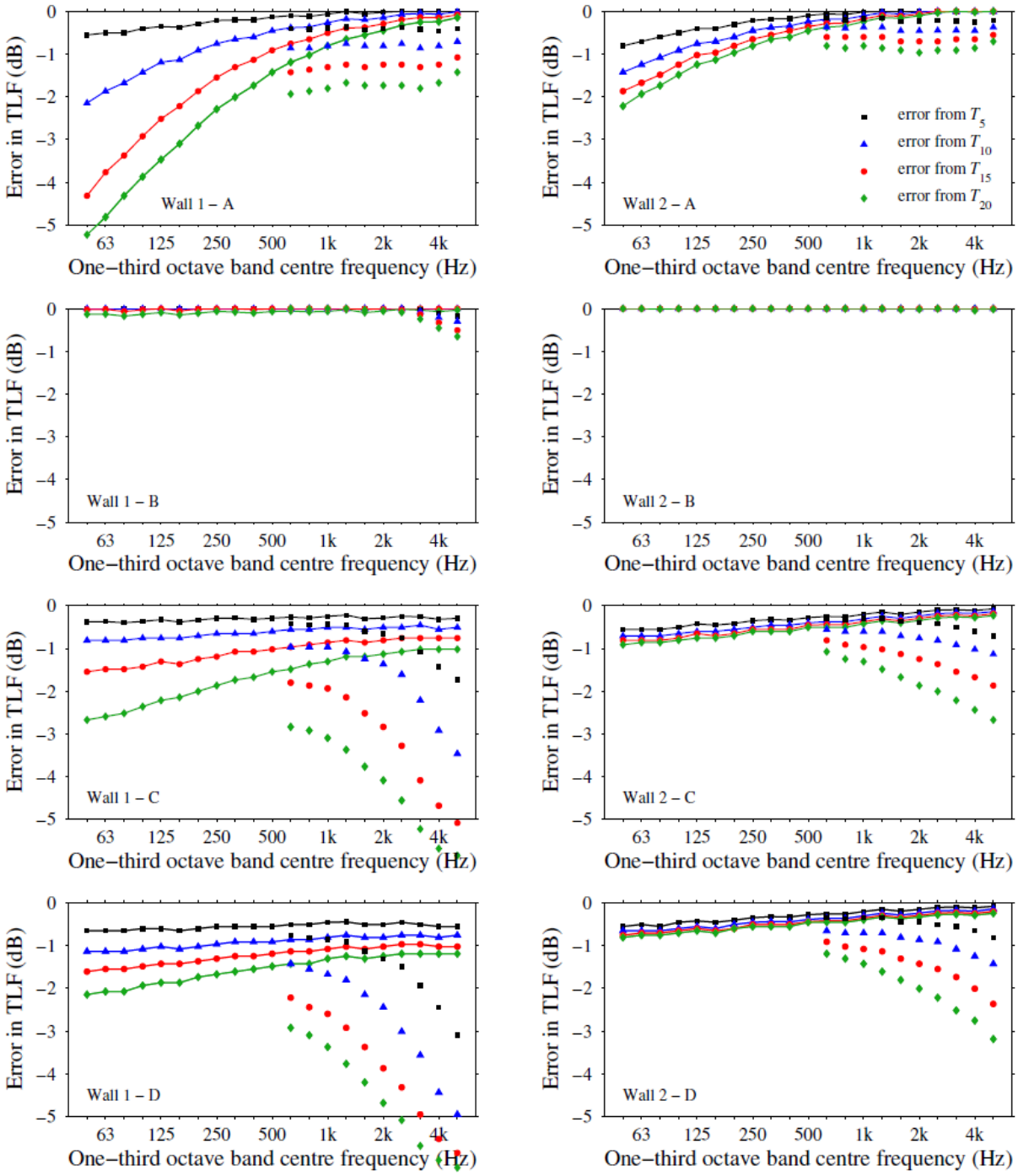

Figure 11. Errors in the total loss factor calculated using structural reverberation times with different evaluation ranges for the T-junction in test arrangements A, B, C and D. Markers connected with solid lines represent the bending only model (50Hz to 5kHz). Markers without lines represent the bending and in-plane model (630Hz to 5kHz).

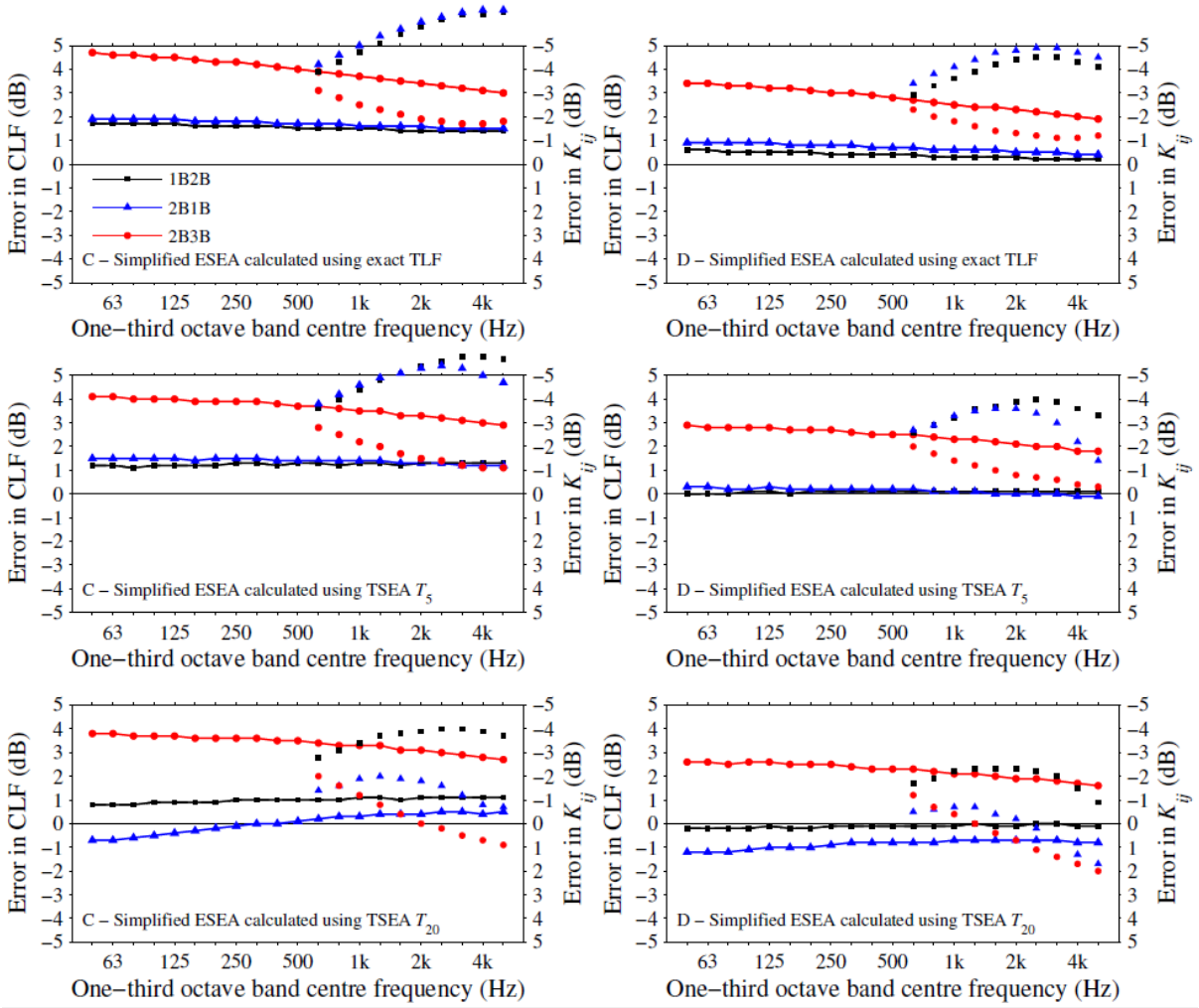

Figure 12. Error in the laboratory measurement of structural coupling parameters, η_{ij} and K_{ij} , for the T-junction in test arrangements C and D when calculated using either the exact TLF or the TLF calculated using T_5 and T_{20} from TSEA. Markers connected with solid lines represent the bending only model (50Hz to 5kHz). Markers without lines represent the bending and in-plane model (630Hz to 5kHz).

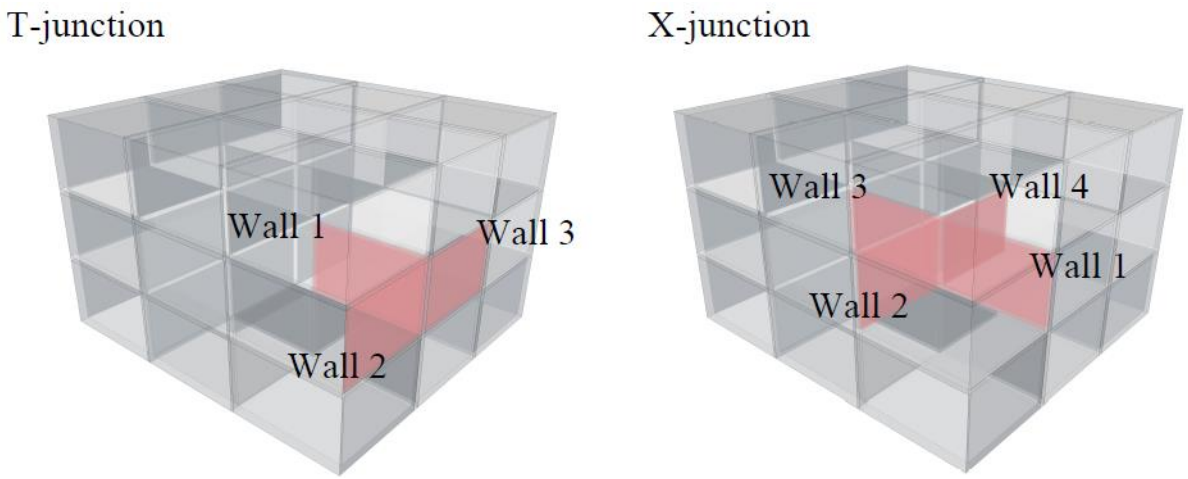

Figure 13. Large building used to simulate the field situation for the measurement of structural coupling parameters with the T-junction and X-junction that are focussed on in the analysis shown in red.

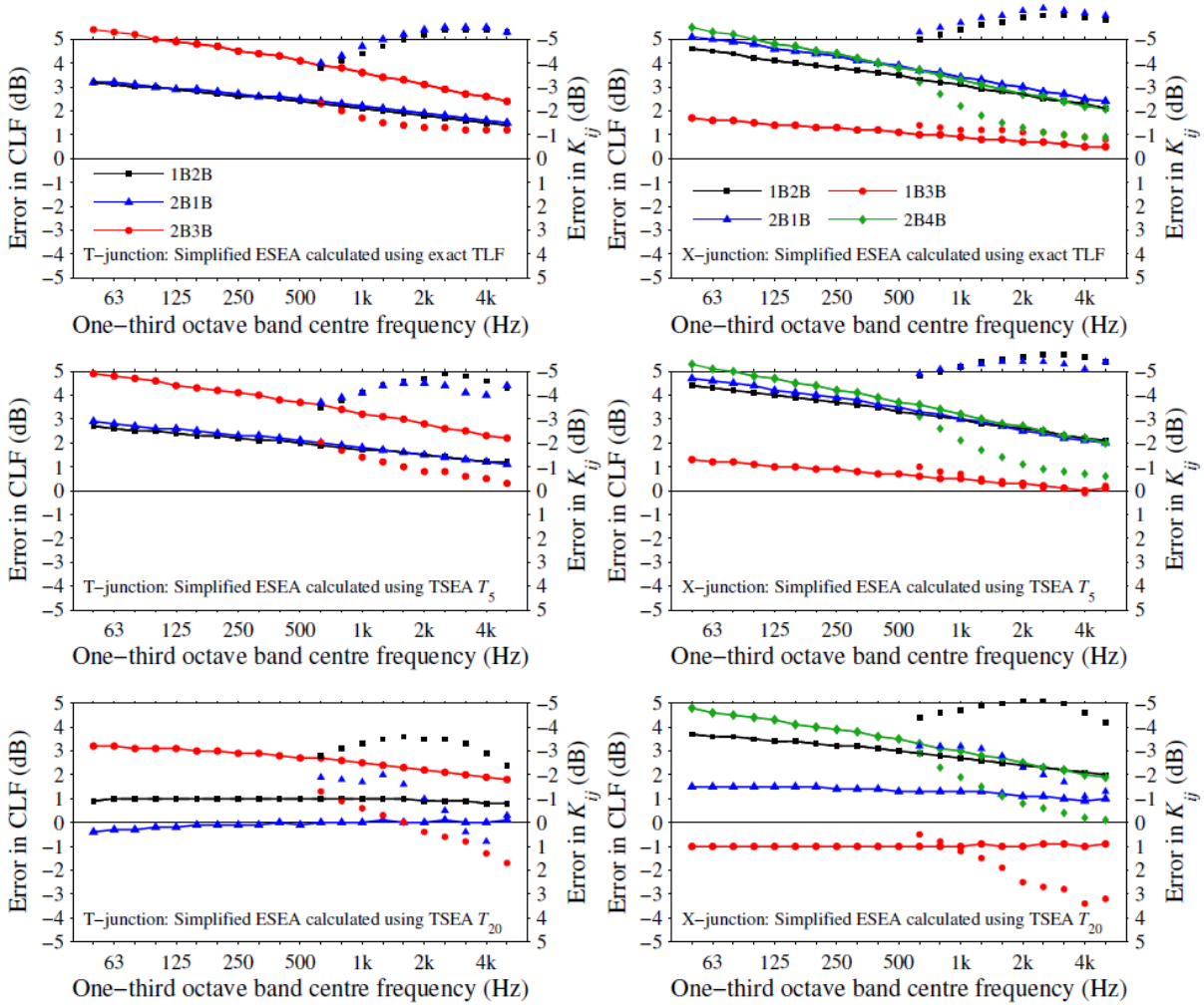

Figure 14. Error in the *in situ* measurement of structural coupling parameters, η_{ij} and K_{ij}, in the large building for the T-junction (left column) and the X-junction (right column) when calculated using either the exact TLF or the TLF calculated using T_5 and T_{20} from TSEA. Markers connected with solid lines represent the bending only model (50Hz to 5kHz). Markers without lines represent the bending and in-plane model (630Hz to 5kHz).

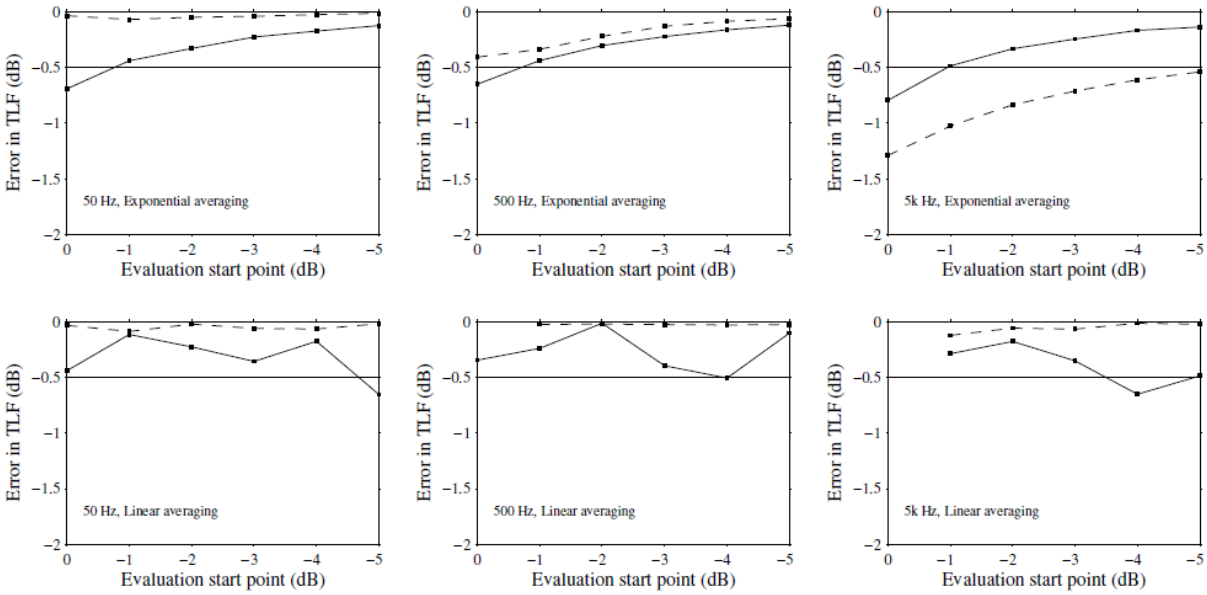

Figure 15. Error in the TLF calculated from T_5 for different evaluation start points using reverse-filter analysis with backwards integration. The errors are shown at 50Hz, 500Hz and 5kHz for a total loss factor of $f^{-0.5}$+0.01. The upper row of graphs show exponential averaging with a time constant of τ=1/1024 (dashed line) and τ=T/30 (solid line). The lower row of graphs show linear averaging with an averaging time of 1ms (dashed line) and T/12 (solid line).

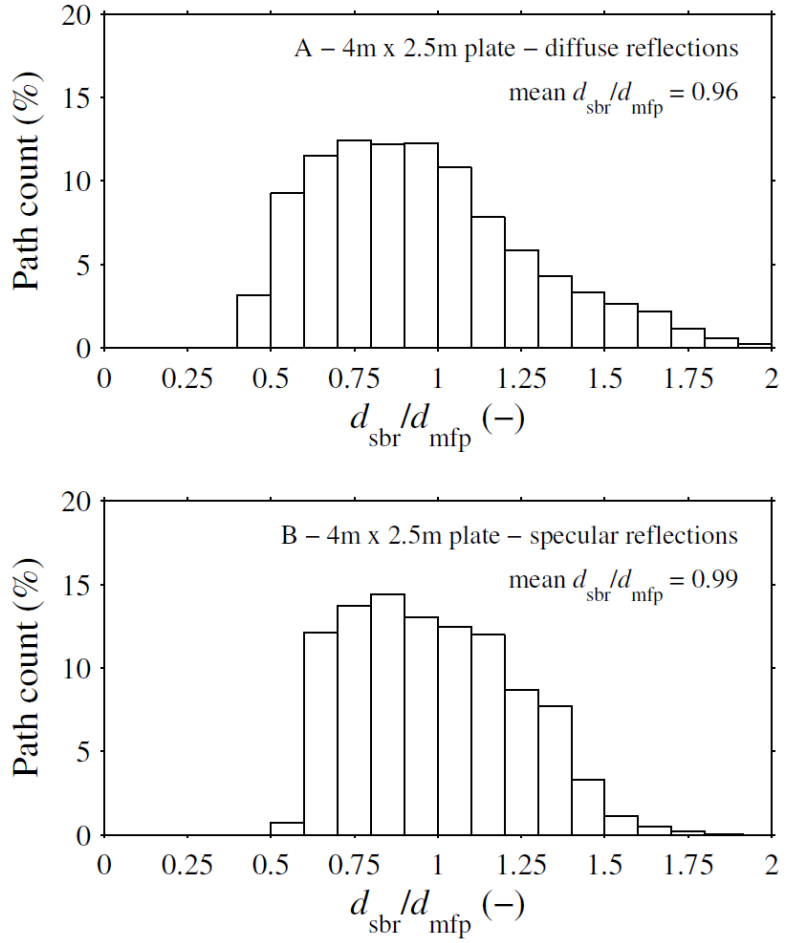

Figure 16. Monte-Carlo simulations of source-to-boundary-to-receiver path distances, d_{sbr}, normalised to the mean free path, d_{mfp} for a point source on a 10m^2 rectangular plate for (a) diffuse reflections and (b) specular reflections at the boundaries.

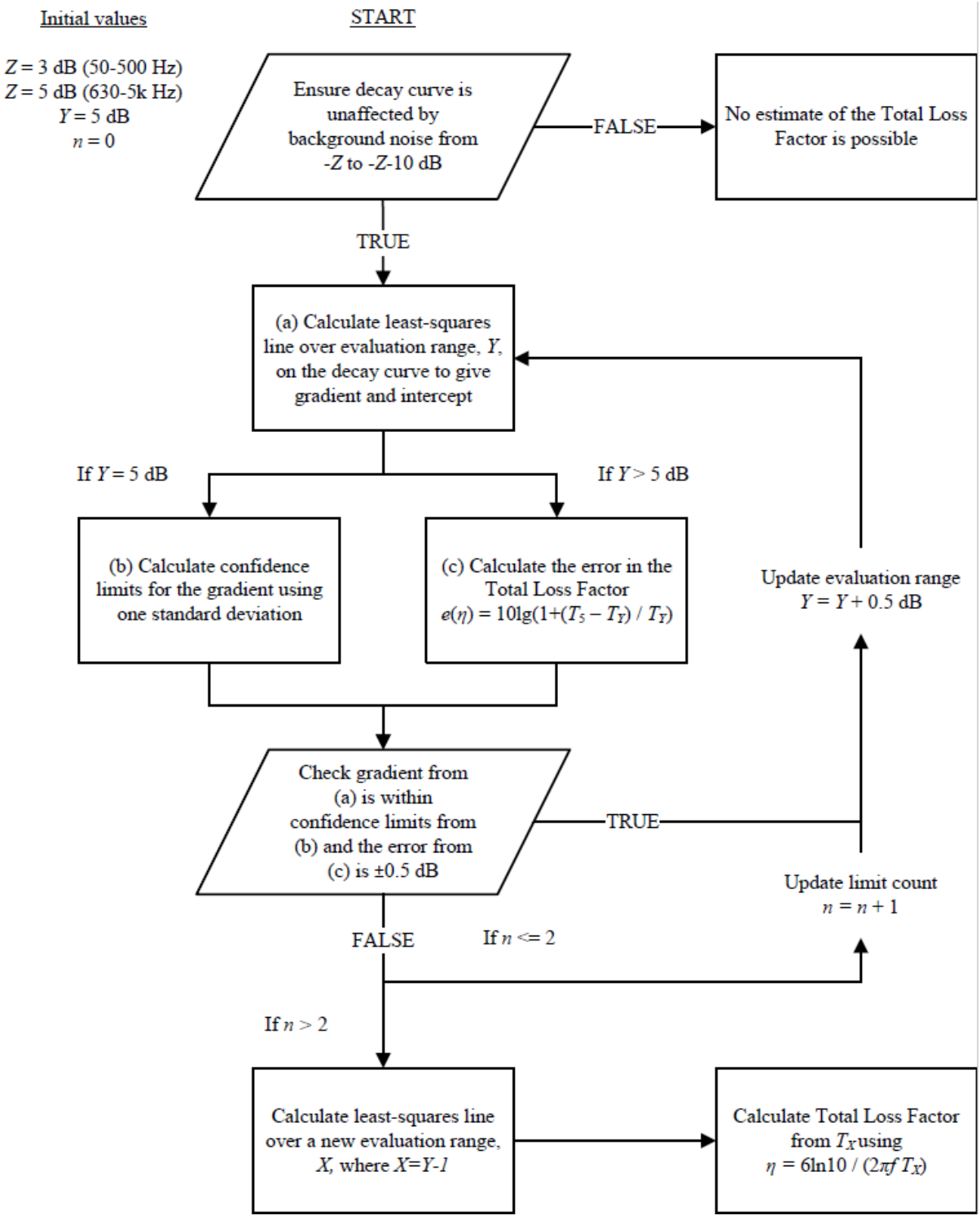

Figure 17. Evaluation procedure for structural reverberation times on heavyweight walls and floors.

References

[1] T. Kihlman and A.C. Nilsson. The effects of some laboratory designs and mounting conditions on reduction index measurements, Journal of Sound and Vibration, 24 (3), 349–364 (1972).

[2] A. Meier, A. Schmitz and G. Raabe. Inter-laboratory test of sound insulation measurements on heavy walls. Part 2 – Results of main test, Building Acoustics, 6 (3/4) (1999) 171–186.

[3] C. Hopkins. Sound insulation. Butterworth-Heinemann, 2007. ISBN 978-0-7506-6526-1.

[4] ISO 10848-1:2006 Acoustics – Laboratory measurement of the flanking transmission of airborne and impact sound between adjoining rooms – Part 1: Frame document, International Organization for Standardization.

[5] C. Kling and W. Scholl. Transient SEA studies on the damping of coupled building elements. Acta Acustica united with Acustica 97, 266-277 (2011).

[6] R.J.M. Craik. Sound transmission through buildings using statistical energy analysis. First ed. Cambridge: Gower; 1996. ISBN: 0566075725.

[7] R.E. Powell and L.R. Quartararo. Statistical energy analysis of transient vibration, American Society of Mechanical Engineers, Winter meeting, Boston, USA, 3-8 (1987).

[8] M. Robinson and C. Hopkins. Transient Statistical Energy Analysis: A two-subsystem model to assess the validity of using steady-state coupling loss factors for plate radiation. Proceedings of International Congress on Sound and Vibration, Brazil (2011).

[9] M. Robinson and C. Hopkins. Prediction of maximum sound pressure and vibration levels in heavyweight building structures using Transient Statistical Energy Analysis. Proceedings of Internoise 2010. Lisbon (2010).

[10] R.H. Lyon, R.G. DeJong. Theory and application of statistical energy analysis (Butterworth-Heinemann, Boston, USA, Second edition, 1995).

[11] F. Jacobsen and J.H. Rindel. Letter to the editor. Time reversed decay measurements, Journal of Sound and Vibration, 117 (1) 187–190 (1987).

[12] C. Hopkins. Vibration transmission between coupled plates using finite element methods and statistical energy analysis. Part 1: Comparison of measured and predicted data for masonry walls with and without apertures, Applied Acoustics, 64, 955–973 (2003).

[13] ISO 10140-5:2010. Acoustics – Laboratory measurement of sound insulation of building elements – Part 5: Requirements for test facilities and equipment, International Organization for Standardization.

[14] C. Hopkins. Experimental statistical energy analysis of coupled plates with wave conversion at the junction. Journal of Sound and Vibration 322, 155-166 (2009).

[15] C. Hopkins. Measurement of the vibration reduction index, Kij , on free-standing masonry wall constructions, Building Acoustics, 6 (3&4) 235–257 (1999).

[16] ISO 3382-1:2009 Acoustics – Measurement of room acoustic parameters – Part 1: Performance spaces, International Organization for Standardization.

[17] J.F. Kenney. E.S. Keeping, Mathematics of Statistics, Part 1, Third ed., Van Nostrand, Princeton, 1962. ASIN: B0007DWFMQ.

[18] F.S. Acton. Analysis of Straight-Line Data, First ed., Dover, New York, 1966. ISBN: 0-486-61747-5.

[19] C. Chatfield, Statistics for Technology, Third ed., Chapman and Hall, London, 1983. ISBN: 0-412-25340-2.